

Gravitational atoms in the braneworld scenario

Sunil Singh Bohra^{1,*}, Subhodeep Sarkar^{1,2,†} and Anjan Ananda Sen^{1,‡}

¹*Center For Theoretical Physics, Jamia Millia Islamia, New Delhi - 110025, India*

²*Indian Institute of Information Technology, Allahabad, Prayagraj, Uttar Pradesh - 211015, India*

(Dated: December 13, 2023)

General relativity (GR) may be modified by adding an extra warped noncompact spatial dimension such that it is indistinguishable from GR as far as local tests of gravity are concerned. However, such a modified theory of gravity should have intriguing consequences on various aspects of black holes which can help us probe how the presence of an extra dimension affects gravity in the strong field regime, and help us distinguish it from GR. Therefore, we have studied massive scalar perturbations of four-dimensional rotating black holes in the Randall Sundrum II braneworld scenario. These black holes are endowed with a tidal charge that contains information pertaining to the extra spatial dimension in the braneworld model. Such black hole spacetimes are also noteworthy because they permit the black hole's rotation parameter to exceed unity, a possibility strictly forbidden by the general theory of relativity. Consequently, they offer valuable insights into exploring the repercussions of modifications to Einstein's theory through possible future observations. Our approach involves the numerical solution of the perturbed field equations using the continued fractions method. First we ascertain the quasinormal mode spectra of the rotating braneworld black hole. We then thoroughly investigate the existence of quasibound states and the associated superradiant instability. Such a superradiant cloud of bosons around the black hole are called gravitational atoms and are invaluable observational probes of ultralight bosonic particles predicted in various extensions of the Standard Model of particle physics. In comparison to four-dimensional Kerr black hole, we report distinctive signatures of the tidal charge and the rotation parameter, which manifest as signals of the extra dimension on both the quasinormal mode and the formation of gravitational atoms.

I. INTRODUCTION

The first direct detection of gravitational waves emitted during the merger of binary black holes and neutron stars [1–3], along with the recent measurements related to the shadows of supermassive black hole candidates like M87* and Sgr A* located at the center of the Messier 87 and the Milky Way galaxies respectively [4–10] as well as the observation of relativistic effects in the orbits of stars around Sgr A* [11–13], has led to a renaissance in testing gravity in the strong field regime [14–26]. To understand classical gravitational interactions, one usually turns to Einstein's general theory of relativity (GR) which is extremely successful as far as solar system experiments, or weak gravitational fields, are concerned [27–30]. These recent breakthroughs have now confirmed that the predictions of GR agree with observations to an unprecedented degree even in the strong field regime [11–13, 31–40], adding enormous heft to decades of progress made in this direction [41–44]. In the near future, pulsar timing arrays and space-borne gravitational wave detectors are expected to put GR to even more stringent tests [41, 45–51]. But of course, this whole enterprise is not without its caveats and one must exercise due caution while interpreting the results [43, 52–56].

Moreover, in spite of its tremendous success across various orders of the length scale, there are both theoretical

and observational aspects of general relativity and black holes (BHs) that motivate us to consider alternatives to Einstein's theory. These so called modified theories of gravity are usually invoked to address issues like the existence of spacetime singularities [57–59], the existence of Cauchy horizons and the breakdown of determinism in GR [60–69], the information loss paradox [70–72], explain the accelerated expansion of the universe [73–77], or the behaviour of galactic rotation curves [78, 79]. But when it comes to modifying gravity, we seem to be limited only by our imagination [43, 80–83]. However such alternative theories must be at par with GR when it comes to satisfying tests of gravity, both in the local and strong field regime, which is a tall order. We now know that it is indeed possible to consistently modify the Einstein-Hilbert action such that we end up with theories which can address one or more of these issues while keeping the local physics unchanged. Some popular alternatives to GR include $f(R)$ theories [84, 85], Lanczos-Lovelock models [86], bimetric gravity [87–89], Horndeski [90–92] and generalized Proca theories [93–95].

In the present work, we focus on one such modification to Einstein's theory which incorporates the presence of a warped extra spatial dimension¹, the so-called braneworld scenario [97–122], and try to infer its imprints

* sunilsinghbohra87@gmail.com

† subhodeep.sarkar1@gmail.com (Corresponding Author)

‡ aaasen@jmi.ac.in

¹ The existence of different kinds of extra spatial dimensions have been invoked by physicists in variety of contexts over the years, starting from the works of Kaluza and Klein [96] in their attempt to unify classical electromagnetism and general relativity. We refer the reader to [97] for a complete account.

in the strong field regime by studying the behaviour of massive scalar field perturbations around a rotating black hole solution of the said modified theory.

Here we specifically consider the Randall-Sundrum braneworld scenario, where we model the universe as a four dimensional ($4D$) spacetime (or a 3-brane) embedded in a five dimensional ($5D$) anti-de Sitter spacetime called the bulk, the extra dimension being spacelike and warped [98, 99]. In such models, the matter fields are confined to the brane and only gravitational interactions can probe the bulk. The braneworld paradigm was initially proposed as a solution to the hierarchy problem in particle physics [98]. However, Randall and Sundrum proposed a second model, colloquially known as the RS-II model [99], where the observable universe is a 3-brane with a positive tension embedded in the $5D$ bulk spacetime with an warped noncompact extra dimension and a negative cosmological constant. It is particularly interesting to note that such a model can give rise to the familiar Newtonian gravitational potential on the 3-brane [99]. It was also demonstrated that the such a theory is able to reproduce the features of $4D$ Einstein gravity in the low energy limit [102–107] and numerical black hole solutions in the bulk were explored in [101]. Interestingly enough, the RS-II model can also give rise to analytical black hole solutions on the brane [110, 111] that at first sight look superficially familiar to the well known black hole solutions in general relativity, and to understand this aspect we must look at how one arrives at the braneworld black hole metric which is a solution to the (effective) Einstein field equations on the brane [102–105].

Now, in order to construct black hole solutions localized on the brane, one starts with the assumption that the $5D$ Einstein field equations are satisfied by the bulk spacetime. Then, by using an appropriate projector to the brane, and the Gauss-Codazzi relations, one can figure out the $4D$ Einstein tensor on the brane. In fact, if the bulk spacetime is empty and there are no matter fields present on the brane, then the effective gravitational field equations on the brane are given by [102–105]

$${}^{(4)}R_{\mu\nu} = -E_{\mu\nu}, \quad {}^{(4)}R_{\mu}^{\mu} = E_{\mu}^{\mu} = 0, \quad (1.1)$$

where ${}^{(4)}R_{\mu\nu}$ is the $4D$ Ricci tensor and $E_{\mu\nu}$ is traceless electric part of the $5D$ Weyl tensor. Therefore, from (1.1) it is clear that it is the bulk Weyl tensor that ushers in the modifications to the vacuum Einstein field equations due to the presence of the extra spatial dimension [102, 105, 109]. Now, one can show that $E_{\mu\nu}$ is divergenceless as well if one considers a vacuum brane [105]. Therefore the effective vacuum braneworld field equations closely resemble those of the Einstein-Maxwell system. Dadhich *et al.* [110] used this observation to consistently map the Reissner-Nordstöm solution in GR to an exact static spherically symmetric black hole solution localised on a brane, and soon afterwards the technique was generalized to construct a stationary and axisymmetric solution of the vacuum braneworld field equations describing a charged rotating black hole localized on a

3-brane [111], the charge being an induced *tidal charge*, inherited from the $5D$ Weyl tensor, encoding nonlocal gravitational effects from the higher dimensional bulk spacetime.

So, the rotating braneworld BH metric resembles that of the the Kerr-Newman (KN) black hole [111], and in light of the discussion so far it hardly surprising in hindsight. But the solution is far from trivial and has an important implication since, unlike the KN solution, the braneworld solution corresponds to a vacuum solution, and the tidal charge, bearing the signature of the extra dimension, can take on both positive and negative values (unlike the electric charge). It is also important to stress that unlike KN BHs of general relativity, the braneworld BH can be *superspinning*, that is, they can possess angular momentum greater than the BH mass. Note that the black holes in our universe are supposed to be electrically neutral. But even then electrically charged black holes are routinely studied because they serve as theoretical laboratories to probe various classical and quantum aspects of gravity [123]. Therefore, by using the braneworld BH solution, one can often directly leverage existing techniques to investigate the consequences of the braneworld scenario in the context of gravitational interactions. Such an endeavour is important because it will complement the popular program to search for extra dimensions through particle physics experiments which may be inadequate to probe the presence of the noncompact extra dimension built into the RS-II model [124]. Against this backdrop, workers have studied the imprint of the tidal charge on lensing and BH shadows [125–132], BH perturbations and gravitational waves [133–148], and have explored various other aspects [149–156] as well. In this work, we choose to explore two hitherto unexplored avenues: i) the quasinormal mode spectra of massive perturbation, and ii) the existence of quasibound states or braneworld gravitational atoms and the associated superradiant instability.

Since the seminal work of Vishveshwara [157], quasinormal modes (QNMs), or the characteristic frequencies, of black holes have become ubiquitous to BH physics [158, 159]. These modes are triggered by the presence of perturbing fields near the vicinity of the black hole, or due to perturbations to the background metric itself. Now, because of the existence of the event horizon, a black hole functions as a leaky system. Consequently, the characteristic frequencies (or QNMs) are complex numbers, in contrast to the typical normal modes encountered in the study of conservative systems. They are, in fact, crucial to assessing the stability of the black hole itself, for if the BH is stable under external perturbation then these modes will have to eventually decay as they radiate through the horizon and infinity. The importance of QNMs also lie in the fact that these modes are completely determined by the black hole parameters like mass M , charge Q , angular momentum J , the spin of the perturbing field, and the geometry of the spacetime: they remain independent of the initial perturbation

that excites them, thereby carrying a unique fingerprint of the black hole spacetime. While gravitational perturbations are pivotal from an observational standpoint, the study of massive scalar perturbations is important in its own right [42, 160]. Setting aside the fact that studying the quasinormal mode spectrum of fields of different spins is the first step towards assessing the stability of the BH, massive scalar fields can act as a useful proxy for more realistic baryonic fields. Hence they act as a useful precursor to full-scale numerical relativity simulations. Furthermore, in asymptotically flat spacetimes, the presence of the scalar field mass fundamentally alters the behaviour of the scattering potential at infinity since it now asymptotes to a constant value. This feature leads to an interesting behaviour in certain QNM frequencies which can become arbitrarily long lived, giving rise to the phenomena called *quasiresonance*. Moreover, the massive scalar field potential is now able to trap certain modes since due to the presence of a mass barrier, the radial effective potential acts as a reflecting surface. Such modes, called quasibound states, decay exponentially near infinity (in contrast to QNM, even though they still leak away through the horizon) and can be extremely long-lived. In fact, these modes can further extract mass and angular momentum from a rotating BH through the familiar superradiance mechanism [160] and become *superradiantly unstable* due to successive reflections from the potential barrier, leading to the growth of a scalar condensate outside the BH horizon. Such configurations are similar to the so-called *black hole bombs* [161, 162]. In the non-relativistic limit, these black hole systems carrying a *boson cloud* are also called gravitational atoms since the system loosely resembles that of a hydrogen atom [163–169]. Such gravitational atoms can be an invaluable tool when it comes to probing the existence of ultralight bosons beyond the Standard Model of particle physics [163–169]. Recently, a relativistic framework for studying boson clouds has been proposed as well [170].

The massive scalar field propagating in the Kerr and Kerr Newman background has received a lot of attention over the last ~ 50 years since the pioneering studies of Damour, Deruelle and Ruffini [171], Zouros and Eardley [172], and Detweiler [173], and it continues to be an active area of investigation given its rich phenomenology in light of strong field tests of GR; an excellent description of both the history and the physics of the subject can be found in [160]. In recent times, it is worth mentioning that the QNM spectrum of massive scalar fields for Kerr and Kerr Newman black holes were studied in [174, 175] using the method of continued fractions developed by Leaver [176]. Studies focusing on the instability of the massive scalar field, or the gravitational atom, in the Kerr background was carried out in [177–181], the same for the Kerr Newman black hole was explored in [182–185]. Similar studies have been carried out for Kerr-like black holes [186] and galactic black holes as well [187].

In the context of braneworld BHs, massless scalar

and gravitational QNMs were studied in [133, 134] for the spherically symmetric case. The gravitational QNM spectrum for the rotating case has been investigated in [188, 189]. In these studies, the authors tried to constrain the value of the tidal charge using gravitational wave data. But it seems that current observations are unable to strongly discriminate between GR and the braneworld scenario. The effect of the tidal charge on superradiance was recently studied in [143] by analyzing the amplification factors of massless scalar waves being scattered by the black hole. However, for massive scalar fields, the analysis has been limited to analytical examinations of extremal configurations [147] where some interesting bounds were obtained on the tidal charge and the BH parameters that ensured that the configuration is super-radiantly stable.

In the present work, we initiate a numerical exploration of the massive scalar quasinormal mode and quasibound state spectra of rotating braneworld BHs. We focus in the regime $\mu M < 1$ such that one obtains boson condensates around black hole forming a scalar gravitational atom, μ being the mass of the scalar field and M being the BH mass that sets a characteristic length scale of the problem. The paper is organised as follows. In Section II we introduce the rotating braneworld BH metric and discuss the region of the parameter space under exploration. In Section III, we discuss the wave equation governing massive scalar perturbation and elucidate the boundary conditions required for studying quasinormal modes and quasibound states. We then discuss the numerical method in Section IV and delineate a strategy to solve the continued fraction using a simple root finding algorithm that guarantees results up to the desired degree of accuracy. We present our results in Section V where we first analyze the stability of the braneworld BH under massive scalar perturbations, highlighting interesting aspects of the QNM spectrum, followed by a thorough analysis of the superradiant instability and the braneworld gravitational atom. Finally we conclude with a few remarks in VI.

Notations and conventions: We set the fundamental constants G and c to unity. Throughout this paper, we will use the mostly positive signature convention, such that the Minkowski spacetime will have the metric $\eta_{\nu\mu} = \text{diag}(-1, 1, 1, 1)$. In our numerical computations, we set the characteristic length scale given by the BH mass M to unity.

II. ROTATING BLACK HOLE IN THE BRANEWORLD SCENARIO

Formally, the line element for a rotating black hole in the second Randall-Sundrum (RS-II) braneworld scenario [111–113], with mass M and angular momentum $J \equiv aM$ in the usual Boyer-Lindquist coordinates, is

given by,

$$ds^2 = -\frac{\Delta}{\Sigma} (dt - a \sin^2 \theta)^2 + \Sigma \left(\frac{dr^2}{\Delta} + d\theta^2 \right) + \frac{\sin^2 \theta}{\Sigma} (adt - (r^2 + a^2)d\phi)^2, \quad (2.1)$$

where the metric functions Δ and Σ have the form,

$$\Delta = r^2 + a^2 - 2Mr - \beta, \quad \text{and } \Sigma = r^2 + a^2 \cos^2 \theta, \quad (2.2)$$

and β is the tidal charge inherited from the bulk Weyl tensor. The tidal charge β appears in the metric even though there is no electric charge on the brane and its origin lies in non-local Coulomb-type effects present in the bulk space [110, 111]. It is important to note that β can take on both positive and negative values, and it is evident that for negative values of β , the line element (2.1) resembles the standard Kerr-Newman (KN) solution of the Einstein field equations in general relativity (GR)², and for $\beta = 0$ we simply recover the celebrated Kerr solution. Therefore, positive values of β differentiates this black hole solution from the standard solutions in general relativity and carries the imprint of extra dimensions. In fact, in the context of braneworld models, a positive value of β is physically more favourable [101, 102, 108]. We should also stress that the tidal charge is a property of the spacetime geometry itself and is different from a black hole hair, which is to say that it is similar to how the cosmological constant is a property of an asymptotically de Sitter black hole spacetime and has the same value for all such black holes, whereas a black hole hair like the mass M , or electric charge Q can be different for different black holes in the universe. The rotating braneworld black hole is therefore clearly quite distinct from its GR counter part despite the superficial similarity. Moreover, the presence of the tidal charge β permits us to explore those values of the black hole rotation parameter a that are not allowed in GR. This fact is evident from examining the roots of $\Delta(r) = (r - r_+)(r - r_-) = 0$, viz.,

$$r_{\pm} = M \pm k, \quad (2.3)$$

where $k \equiv \sqrt{M^2 - a^2 + \beta}$.

The black hole will have an outer event horizon described by the largest root r_+ provided,

$$(a/M)^2 \leq 1 + \beta/M^2, \quad (2.4)$$

where the equality in the above relation corresponds to the case where $r_+ = r_- = M$, that is, in the extremal limit when the two horizons will coincide. The violation

of (2.4) results in a spacetime harbouring a naked singularity. Now, for the BH to achieve extremality, it is evident that for positive values of β , we must allow for the possibility $a/M \geq 1$, a situation that is forbidden for black holes in Einstein's general theory of relativity and hence one that is not discussed while studying rotating black holes in GR. Therefore to explore effects arising out of modifications to general relativity, one has to explore the regime where the rotation parameter a is greater than the mass M of the black hole in presence of a tidal charge $\beta > 0$. Furthermore, to guarantee the existence of an inner horizon r_- , according to (2.3), one must ensure that

$$M > k \implies \beta < a^2. \quad (2.5)$$

If (2.5) is not satisfied, the spacetime would still describe a rotating black hole but with only one horizon, a geometry whose global structure would be quite different from that of the usual Kerr black hole. We shall therefore restrict our investigation to those black hole geometries which have an inner and outer horizon, that is, focus on values of β satisfying,

$$(a/M)^2 - 1 \leq \beta/M^2 < (a/M)^2. \quad (2.6)$$

In Fig. 1, we have shown the portion of the parameter space spanned by the allowed values a and β in the RS-II braneworld scenario (keeping in mind (2.6)), and compared it with the region described by the KN solution in general relativity. Note that a and β are theoretically unbounded from above. We have also indicated the values of a and β which satisfy the equality in (2.4) by a thick dotted black curve. We term this as the *extremal curve*, and later on we shall call the modes corresponding to a and β lying close to this curve as near-extremal modes. It is evident that the braneworld black hole provides us with an opportunity to explore a much larger portion of the parameter space compared to GR and hence allows us to investigate the imprint of an otherwise hidden extra dimension on various physical phenomena.

III. MASSIVE SCALAR PERTURBATIONS AROUND THE ROTATING BRANEWORLD BACKGROUND

The chief motivation of the present work is to study the behavior of (massive) scalar field perturbations propagating in the rotating braneworld BH background. Studying such perturbations help us probe various properties of the background spacetime since they are completely determined by the background geometry. The derivation of the concerned equations and boundary condition is operationally identical to that of massive scalar perturbations in the KN background. We therefore only highlight the major steps and results. We start by considering a test field $\psi(t, r, \theta, \phi)$ of mass μ satisfying the Klein-Gordon (KG) equation.

$$\frac{1}{\sqrt{-g}} \partial_{\mu} (g^{\mu\nu} \sqrt{-g} \partial_{\nu} \psi) - \mu^2 \psi = 0, \quad (3.1)$$

² The reader should note that our convention is different from [111–113]. In their notation, $\Delta = r^2 + a^2 - 2Mr + \beta$. So, in their case, a positive value of β corresponds to the KN black hole.

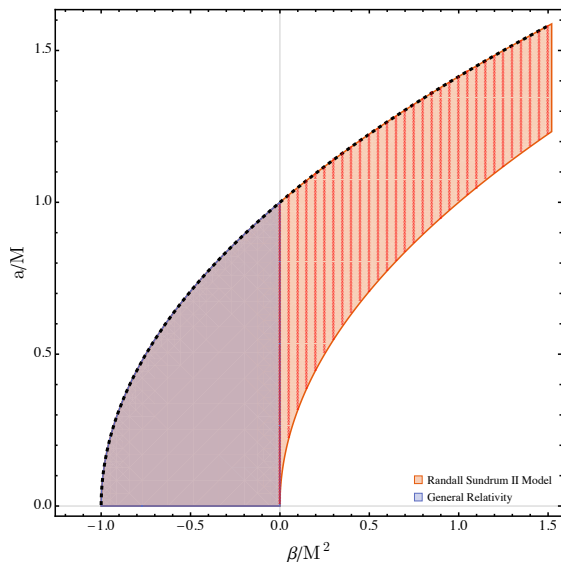


FIG. 1. The space of values of BH spin a and tidal charge β which ensure that the rotating braneworld black hole possesses two horizons is shown in orange. The blue region shows the allowed values of a and β in the Kerr-Newman spacetime provided $\beta = -Q^2$ is interpreted as the usual electric charge. Although the two solutions are fundamentally different, the braneworld BH being a vacuum solution, they are operationally indistinguishable in the region of overlap ($\beta < 0$). The red cross-marks in the parameter space indicates values of a and β sampled to compute the quasinormal modes in the text, and extremal values of a and β lie on the thick dotted black curve.

where g is the determinant of the metric given by (2.1), and we assume that the test field does not backreact on the background [158, 159]. Since the metric (2.1) possesses Killing vectors ∂_t and ∂_ϕ , the wave equation (3.1) can be solved by the method of separation of variables, using the *ansatz*,

$$\psi(t, r, \theta, \phi) = e^{-i\omega t + im\phi} S_{lm}(\theta) R_{lm}(r), \quad (3.2)$$

where we have introduced the frequency ω and $m \in \mathbb{Z}$ is the azimuthal number. Using the *ansatz* (3.2), we can separate out the KG equation (3.1) into two coupled ordinary differential equations (ODEs) satisfied by the angular and the radial eigenfunctions, $S_{lm}(\theta)$ and $R_{lm}(r)$ respectively. We therefore find that $S_{lm}(\theta)$ satisfies

$$\frac{1}{\sin \theta} \frac{d}{d\theta} \left(\sin \theta \frac{dS_{lm}(\theta)}{d\theta} \right) + \left(a^2(\omega^2 - \mu^2) \cos^2 \theta - \frac{m^2}{\sin^2 \theta} + A_{lm} \right) S_{lm}(\theta) = 0, \quad (3.3)$$

where A_{lm} is the separation constant of the problem, and (3.3) is known as the standard oblate spheroidal harmonic equation. In the limit $a \rightarrow 0$, $S_{lm} \rightarrow Y_{lm}$ where Y_{lm} denote the familiar spherical harmonics, and

$A_{lm} \rightarrow l(l+1)$, where l is a non-negative integer and in the static limit it can be identified with the angular number or the order of Y_{lm} . Therefore l can also be used to indicate the order of the spheroidal harmonic S_{lm} and to label the modes. Note that by introducing a new variable, $u = \cos \theta$ with the range u is $-1 \leq u \leq 1$, (3.3) can be transformed to the following form

$$(1-u^2) \frac{dS_{lm}(u)}{du} - 2u \frac{dS_{lm}(u)}{du} + \left(\bar{\Lambda} + \gamma^2 - \gamma^2 u^2 - \frac{m^2}{1-u^2} \right) S_{lm}(u) = 0, \quad (3.4)$$

where we have introduced the constants γ and $\bar{\Lambda}$ such that $\gamma = ia\sqrt{\omega^2 - \mu^2}$ and $A_{lm} = \gamma^2 + \bar{\Lambda}$. We note that the regularity of $S_{lm}(u)$ at $u = \pm 1$ demands $m = 0, \pm 1, \pm 2, \dots, \pm l$.

We can also show that the radial eigenfunction $R_{lm}(r)$ satisfies,

$$\Delta \frac{d}{dr} \left(\Delta \frac{dR_{lm}(r)}{dr} \right) + U_{lm}(r) R_{lm}(r) = 0, \quad (3.5)$$

where

$$U_{lm}(r) = K^2 - \Delta(\lambda_{lm} + r^2\mu^2), \quad (3.6)$$

with $\lambda_{lm} = A_{lm} + a^2\omega^2 - 2am\omega$, $K = \omega(r^2 + a^2) - am$ and $\Delta = (r - r_+)(r - r_-)$.

We see that although (3.1) is separable, the two ODEs (3.3) and (3.5) that we have obtained are coupled and therefore to solve the eigenvalue problem, we need to solve the two equations simultaneously to determine the separation constant A_{lm} and the eigenfrequencies ω . We have to also supplement equations (3.3) and (3.5) with suitable boundary conditions (BCs) dictated by the physics of the problem which we shall now discuss.

A. Boundary conditions, quasinormal modes and quasibound states

To determine the appropriate boundary conditions required study massive scalar perturbations, we introduce the radial function $\bar{R}_{lm} = \sqrt{r^2 + a^2} R_{lm}$ and the tortoise coordinate in the usual manner, viz.,

$$dr_* = \frac{r^2 + a^2}{\Delta} dr, \quad (3.7)$$

and rewrite the radial equation (3.5) as,

$$\frac{d^2 \bar{R}_{lm}}{dr_*^2} + \bar{U}_{lm} \bar{R}_{lm} = 0, \quad (3.8)$$

where

$$\bar{U}_{lm} = (\omega - \omega_c)^2 - \frac{\Delta}{(r^2 + a^2)^2} (\lambda_{lm} + H(r)), \quad (3.9)$$

with,

$$\omega_c = \frac{am}{r_+^2 + a^2}, \quad (3.10)$$

and

$$H(r) = r^2 \mu^2 + \frac{(r\Delta)'}{r^2 + a^2} - \frac{3\Delta r^2}{(r^2 + a^2)^2}. \quad (3.11)$$

Here prime denotes a derivative with respect to r , and the resultant equation (3.8) resembles Schrödinger equation.

Now due to the presence of the event horizon at $r = r_+$, the black hole system is inherently dissipative or non-conservative: waves that fall into the black hole carry energy out of the system and by the virtue of the definition of an event horizon in classical gravity, nothing can emerge from the event horizon as well. Therefore the scalar waves must satisfy perfectly ingoing boundary conditions at the horizon. To figure out the form of the boundary condition near the horizon, we need to solve (3.8) asymptotically as $r \rightarrow r_+$, or $r_* \rightarrow -\infty$, such that $\Delta(r_+) \sim 0$, which in turn implies $\bar{U}_{lm} \sim (\omega - \omega_c)^2$. Noting that near r_+ , we can write

$$r_* \sim \frac{r_+^2 + a^2}{r_+ - r_-} \ln(r - r_+),$$

we find that a solution that is purely ingoing at the event horizon in $v = t + r_*$ coordinates is given by,

$$R_{lm}(r \rightarrow r_+) \sim e^{-i(\omega - \omega_c)r_*} \sim (r - r_+)^{-i\delta}, \quad (3.12)$$

where

$$\delta = \frac{(r_+^2 + a^2)\omega - am}{r_+ - r_-}.$$

Now, depending on the boundary condition we choose to impose at $r \rightarrow \infty$, we can have different solutions to the eigenvalue problem specified by (3.8). In addition to the purely ingoing BC at r_+ , if we demand that the modes are perfectly outgoing at infinity, we would obtain the *quasinormal modes* (QNMs) of the black hole. However, if the boundary condition is such that the modes decay exponentially near infinity, we get the *quasibound states* (QBSs) of the spacetime. Note that as $r \rightarrow \infty$, or $r_* \rightarrow \infty$, the potential (3.9) reduces to

$$\bar{U}_{lm} \sim \omega^2 - \mu^2 + \mu^2 \frac{(r_+ + r_-)}{r}, \quad (3.13)$$

and hence we can find an asymptotic solution to (3.8) near infinity to obtain [186, 190, 191],

$$\begin{aligned} R_{lm}(r \rightarrow \infty) &\sim r^{i(r_+ + r_-)\mu^2/2\Omega - 1} e^{i\Omega r_*}, \\ &\sim r^{i\rho - 1} e^{q r}, \end{aligned} \quad (3.14)$$

where,

$$\rho = \left(\frac{2\omega^2 - \mu^2}{2\Omega} \right) (r_+ + r_-), \quad (3.15)$$

$$\Omega = \pm \sqrt{\omega^2 - \mu^2}, \quad (3.16)$$

$$q = i\Omega = \pm \sqrt{\mu^2 - \omega^2}. \quad (3.17)$$

Note that while obtaining (3.14), we have consistently taken into account the contribution from the subleading terms near infinity, this is important to ensure the accuracy of the continued fraction method discussed in the next section [190]. It is also interesting to note that (3.14) enables us to study QNMs and QBSs in an unified manner, based on our choice of the sign of q in (3.17). If $\text{Re}(q) > 0$, then the solution diverges near $r \rightarrow \infty$ and it is consistent with purely outgoing boundary conditions at infinity. Hence $\text{Re}(q) > 0$ is suitable for studying QNMs. On the other hand, the solution exponentially vanishes near infinity for $\text{Re}(q) < 0$, and hence such a choice is suitable for studying QBS [178, 184]. The eigenfrequencies ω that we shall compute are in general complex, that is $\omega = \omega_R + i\omega_I$, unlike the normal mode frequencies of conservative system, and is therefore a hallmark of the dissipative nature of the system due to the loss of energy through the horizon (and also through the infinity for QNMs). The real part of the frequency, $\text{Re}(\omega)$ represents the frequency of oscillation and the imaginary part $\text{Im}(\omega)$ represents the rate of growth or decay of the perturbation. While studying QNMs, for stable perturbations that decay with time, $\text{Im}(\omega) < 0$ and $|\text{Im}(\omega)|$ can be identified with the decay rate. Since we are studying massive scalar field perturbations, the quasibound states may be prone to superradiant instabilities. Such modes are characterised by $\text{Im}(\omega) > 0$ and it represents the rate of growth of the instability. Furthermore, the oscillation frequency of these modes is supposed to satisfy [180, 183, 192]

$$0 < \text{Re}(\omega) < \mu, \text{ and } 0 < \text{Re}(\omega) < \omega_c. \quad (3.18)$$

The first of the above two conditions ensures that the modes are reflected from the potential barrier at infinity while the second one is the usual condition for superradiance. These two condition together ensure the growth of the superradiant instability and formation of the gravitational atom.

IV. A NUMERICAL RECIPE FOR LEAVER'S METHOD OF CONTINUED FRACTIONS

Armed with (3.4), (3.5), and the boundary conditions (3.12) and (3.14), we now attempt to numerically determine the QNMs and QBSs of the braneworld BH. We have chosen the method of continued fractions proposed by Leaver [176] to compute QNMs. The method itself was first used by Jaffé to compute the electronic spectra of hydrogen molecular ion, and over the years it has been widely used to compute the QNMs and QBS of various black hole geometries and neutron stars. We shall first write down the necessary recurrence relations which resemble those of the KN black hole, and then discuss a strategy to scan the parameter space (c.f.:Fig. 1) in a manner that assures convergence.

A. Radial equation

We begin by considering the following *ansatz* for the radial differential equation that takes into account the BCs (3.12) and (3.14), viz.,

$$R_{lm}(r) = e^{i\Omega r} \left(\frac{r-r_+}{r-r_-} \right)^{i\delta} (r-r_-)^{i\rho} P(r), \quad (4.1)$$

where

$$P(x) = \sum_{n=0}^{\infty} d_n \left(\frac{r-r_+}{r-r_-} \right)^n.$$

We then plug in (4.1) into (3.5) to obtain a three term recurrence relation satisfied by the coefficients a_n , namely,

$$\alpha_0^r a_1 + \beta_0^r a_0 = 0, \quad (4.2)$$

$$\alpha_n^r d_{n+1} + \beta_n^r d_n + \gamma_n^r d_{n-1} = 0, \quad (4.3)$$

with

$$\alpha_n^r = n^2 + (c_0 + 1)n + c_0, \quad (4.4a)$$

$$\beta_n^r = -2n^2 + (c_1 + 2)n + c_3, \quad (4.4b)$$

$$\gamma_n^r = n^2 + (c_2 - 3)n + c_4 - c_2 + 2, \quad (4.4c)$$

and

$$c_0 = 1 + \frac{2i}{(r_+ - r_-)} (am - \omega(a^2 + r_+^2)), \quad (4.5a)$$

$$c_1 = -2(c_0 + 1) + 4ir_+ \Omega + \frac{i\mu^2(r_+ + r_-)}{\Omega}, \quad (4.5b)$$

$$c_2 = c_0 + 2 - i(r_+ + r_-) \left(\frac{2\omega^2 - \mu^2}{\Omega} \right), \quad (4.5c)$$

$$c_3 = c_0 \left[c_0 + \frac{c_1}{2} + i\omega(r_+ + r_-) \right] - i\omega(r_+ + r_-) + a^2\omega^2 + r_+^2(2\omega^2 - \mu^2) - A_{lm}, \quad (4.5d)$$

$$c_4 = c_0 - i(r_+ + r_-)(c_0 - 1)\omega - \frac{(r_+ + r_-)^2\mu^4}{4\Omega^2} - i(r_+ + r_-)(c_0 + 1) \frac{(2\omega^2 - \mu^2)}{2\Omega}. \quad (4.5e)$$

We now divide the (4.3) by d_n and then, after a minor rearrangement, obtain

$$\frac{d_n}{d_{n-1}} = - \frac{\gamma_n^r}{\beta_n^r + \alpha_n^r \frac{d_{n+1}}{d_n}}. \quad (4.6)$$

Now (4.6) can be cast in the form of an infinite continued fraction by substituting the expression for d_{n+1}/d_n (obtained by replacing n with $n+1$ in (4.6)) back into (4.6), and iterating the process till we obtain,

$$\frac{d_n}{d_{n-1}} = - \frac{\gamma_n^r}{\beta_n^r - \alpha_n^r \frac{\gamma_{n+1}^r}{\beta_{n+1}^r - \alpha_{n+1}^r \frac{\gamma_{n+2}^r}{\beta_{n+2}^r - \dots}}}. \quad (4.7)$$

Putting $n = 1$ in (4.7) and equating it with (4.2) we further get

$$0 = \beta_0^r - \frac{\alpha_0^r \gamma_1^r}{\beta_1^r - \beta_2^r} \dots \frac{\alpha_n^r \gamma_{n+1}^r}{\beta_{n+1}^r} \dots. \quad (4.8)$$

The above continued fraction can be inverted n number of times, yielding

$$\beta_n^r - \frac{\alpha_n^r \gamma_{n+1}^r}{\beta_{n+1}^r} \frac{\alpha_{n+1}^r \gamma_{n+2}^r}{\beta_{n+2}^r} \dots = \frac{\alpha_{n-1}^r \gamma_n^r}{\beta_{n-1}^r} \dots \frac{\alpha_0^r \gamma_1^r}{\beta_0^r}. \quad (4.9)$$

We note that putting $n = 0$ in (4.9) gives back (4.8), provided that for $n < 0$, $\alpha_n = \beta_n = \gamma_n = 0$. If we know the value of the separation constant A_{lm} appearing equation (4.5e), we can truncate the continued fraction at a suitably large value N and solve the algebraic equation using an appropriate root finding algorithm to determine the QNM or QBS frequency ω depending on the sign of Ω (as discussed in the previous section), thereby solving the radial eigenvalue problem. The infinite continued fraction (4.9) in principle has an infinite number of roots, however numerically, the n^{th} inversion gives the n^{th} stable root. So to study the fundamental mode, we have to put $n = 0$ in (4.9). The inverse continued fraction is actually more useful in calculating the overtones.

Since we truncate the continued fraction at some N , the *remainder* of the series $R_N = -d_{N+1}/d_N$ can be approximated following Nollert's prescription [193]. Since R_N satisfies the recurrence relation

$$R_N = - \frac{\gamma_{N+1}^r}{\beta_{N+1}^r - \alpha_{N+1}^r R_{N+1}}, \quad (4.10)$$

we can then expand R_N as a power series, viz.,

$$R_N = \sum_{k=0}^{\infty} C_k N^{-k/2}$$

and then by equating the coefficients of each power of \sqrt{N} to zero, we obtain the first three coefficients as

$$\begin{aligned} C_0 &= -1 \\ C_1 &= \pm \sqrt{-2i\Omega(r_+ - r_-)} \\ C_2 &= \frac{3}{4} + 2i\Omega r_+ + \frac{i\mu^2(r_+ + r_-)}{2\Omega} \end{aligned}$$

Note that the sign of C_1 is chosen in such a way that $\text{Re}(C_1)$ should be positive to ensure convergence. Now for a large value of N , the contribution from the terms following N become very small. So, including terms beyond the N^{th} term should not significantly alter the value of the root the continued fraction. However, rather than simply discarding or selecting an arbitrary value for the remaining part, it is preferable to apply Nollert's prescription since Nollert observed that it is crucial when one attempts to calculate modes whose imaginary parts are much larger than their real part, and as a result improves the overall convergence of Leaver's method.

B. Angular equation

We need to solve the angular equation (3.4) to determine the separation constant A_{lm} by imposing the boundary condition that the function $S_{lm}(u)$ is regular at the poles $u = \pm 1$. Taking this into consideration, the series solution for the angular wave-function takes the form,

$$S_{lm} = e^{i\Omega u} (1+u)^{m/2} (1-u)^{m/2} \sum_{n=0}^{\infty} c_n (1+u)^n, \quad (4.11)$$

Substituting (4.11) into (3.4) yields the following three term recurrence relation

$$\alpha_n^\theta c_{n+1} + \beta_n^\theta c_n + \gamma_n^\theta c_{n-1} = 0, \quad (4.12)$$

where

$$\alpha_n^\theta = 2(n+1)(n+m+1), \quad (4.13a)$$

$$\beta_n^\theta = -n^2 + n(4a\Omega - 2m - 1) + A_{lm} + a^2\Omega^2 + (2a\Omega - m)(m+1), \quad (4.13b)$$

$$\gamma_n^\theta = -2a\Omega(n+m). \quad (4.13c)$$

Although we can solve both the radial and angular equations on an equal footing using Leaver's method, in practice we have found that it is often much more computationally inexpensive to use a suitable library function to compute A_{lm} .

C. Implementation

Since we have transformed the problem of finding out the eigenvalues of the ODEs (3.4) and (3.5) into a problem of finding the roots of an infinite continued fraction (4.9), we can solve (4.9) to determine the eigenfrequency ω by specifying the set of values $B = \{a, \beta, \mu, l, m\}$ along with the number of terms to include in the continued fraction N and a suitable guess value ω_0 for the root-finding algorithm. To use (4.9), we also need to specify n , the number of inversions of the continued fraction (4.8), and since we shall be focusing on the fundamental mode, we set $n = 0$. We also set $M = 1$ as the characteristic length scale which means that all dimensionful quantities are suitably scaled with respect to M .

To ensure convergence of the mode $\omega(B)$ for a set of values specified by B and ω_0 , we adopt the following strategy: we first determine $\omega(B)$ for $N = N_1$, and then increment N by dN and recompute the value of $\omega(B)$. We continue the iteration until N reaches a maximum value N_{\max} , or the relative difference between the values of $\omega(B)$ from two successive iterations falls below a specified tolerance $\epsilon = 10^{-p}$. Symbolically, if $\omega(B; N)$ is the value of the root $\omega(B)$ obtained by keeping N terms in the continued fraction, we break the iteration when

$$\log_{10} \left| 1 - \frac{\omega(B; N + dN)}{\omega(B; N)} \right| < -p. \quad (4.14)$$

In our calculation, we have set $p = 7$, ensuring that our results converge up to six decimal places, unless stated otherwise. The values of $\{N_1, dN, N_{\max}\}$ are so chosen as to ensure that the computation finishes in a feasible amount of time on a workstation while ensuring convergence, e.g.: for the $l = m = 0$ QNMs, we take, $N_1 = 100, dN = 100, N_{\max} = 5000$. We have also noticed that while computing QNMs the continued fraction converges for relative small values of $N \sim 300-600$ when the black hole is far from extremality, but for near-extreme configurations it requires a high value of $N \sim 1000-3000$ on average to ensure that the modes converge to six decimal places. Since the scattering problem in black hole spacetimes is inherently dissipative, the eigenvalue spectrum is prone to numerical instabilities arising from rounding-off errors due to machine precision arithmetic [194], therefore it is customary and prudent to perform intermediate calculations using extended precision. In our work we have therefore set the internal precision to at least $4 \times \text{MachinePrecision}$. The strategy outlined so far is used in the computation of both the QNMs and QBSs.

In order to determine the quasinormal modes, we scan the parameter space Fig. 1 in the following manner: we fix the values of l, m and the mass μ of the scalar field and choose a value of the tidal charge β . Since there is theoretically no restriction on the value of the tidal charge, we restrict ourselves to $\beta \leq \beta_{\max} = 1.5$. We then increment the value of a from 0 to the maximum possible value $a_{\max} = \sqrt{1 + \beta_{\max}}$ in steps of $da = 0.01$, and calculate the corresponding fundamental QNM frequency ω for those values of a given β such that the inequality given by (2.6) is satisfied. For the first allowed value of a given β , we use a value approximately equal to the of the fundamental massless scalar quasinormal mode of a Schwarzschild BH or a slowly rotating Kerr BH ($a = 0.000001$) as the initial guess value ω_0 for the root-finding algorithm³. But for subsequent iterations, we use the value of the mode found in the previous iteration as the new value of ω_0 . This is advantageous because near extremality, we found that the convergence of the root-finding algorithm is extremely sensitive to the choice of ω_0 ; for an ‘‘improper’’ choice of ω_0 , the algorithm may also return a value of ω that corresponds to an overtone instead of the fundamental mode. We repeat the process described so far for other values of β in parallel, and we choose values of β lying between 0 and β_{\max} in steps of $d\beta = 0.05$. The sampled points are shown in Fig. 1 as

³ The initial guess value, or an approximate value of the fundamental mode of the Schwarzschild or the slowly rotating Kerr black hole can itself be estimated by computing the logarithm of the absolute value of right hand side of (4.8) over a suitable region of the complex plane, and checking for which value of $\omega = x + iy$, we get a minimum, since this point will lie close to the root of the continued fraction that we are after. The process can be repeated for two values of N to ensure that the minima is not a numerical artifact.

red crosses.

To compute the quasibound states and the associated superradiant instability, we follow a similar approach but instead of exploring the entire parameter space, we focus on a smaller set of values of a and β and we are more concerned with how the modes behave with respect to variations in μ . So, we fix the values of a, l, m , and choose a set of values of β which satisfies (2.6). Then for each pair of a and β , we calculate the quasibound state starting with $\mu = \mu_{\min}$. We then increment μ in steps of $d\mu$ up to μ_{\max} . For the first iteration, while calculating the QBS for μ_{\min} , we set the real and imaginary part of the guess value to $\text{Re}(\omega_0) = 0.95\mu_{\min}$ and $\text{Im}(\omega_0) = 10^{-8}$ respectively, in accordance with (3.18). In subsequent iterations, we use the value of the QBS computed in the previous step as the new guess value. For quasibound states, the first overtone tends to lie very close to the fundamental mode, and hence the root-finding algorithm might be highly sensitive to the choice of the guess value. In our approach, this difficulty may be ameliorated by choosing a smaller value of $d\mu$. Furthermore, in the regime of the superradiant instability, the imaginary part of the QBS has a very small positive value compare to its real part. Therefore to ensure that the modes do indeed converge, we have to apply the criteria given by (4.14) to both real and imaginary parts of ω separately and simultaneously. We have observed that the real part converges much faster than the imaginary part and hence requires a stricter test.

Lastly, we have validated our approach by confirming that it is able to reproduce existing results related to the quasinormal modes and quasibound states of Kerr and Kerr-Newman black holes [178, 184, 187].

V. NUMERICAL RESULTS

In this section, we shall present the results of our numerical explorations, focusing first on the quasinormal modes, and then on the quasibound states and the associated superradiant instability.

A. Quasinormal mode spectra

The fundamental quasinormal modes of the rotating braneworld black hole has been show in Fig. 2 for various (normalized) values of the tidal charge β , BH spin a , and scalar field mass μ , each subfigure corresponding to different values of l and m . Each curve in the complex plane is labeled by β , and the color of each point corresponds to the value of a , whereas the value of μ is indicated by the shape of the marker. In Fig. 2, we have restricted ourselves to $0 \leq \beta \leq 1$, with the value of a being constrained by (2.6). However, theoretically there is no upper bound on β . Hence we have also explored the $\beta > 1$ regime as well, and to get an idea of how the QNMs behave for different values of β, a, μ , we have

presented contour plots showing how the real and imaginary part of the QNMs vary with respect to a and β for massless and massive perturbations in Fig. 4, and in Fig. 5 and Fig. 6 for $l = 0, 1$ respectively.

For QNMs, recall that $\text{Re}(\omega)$ represents the frequency of oscillation and $|\text{Im}(\omega)|$ stands for the rate of decay of the perturbations. For the $l = m = 0$ modes, we observe from the top left panel of Fig. 2 that $\text{Re}(\omega)$ and $-\text{Im}(\omega)$ decreases if the tidal charge β is increased. If we fix β , then the frequency of oscillation increases with a until it reaches its maximum value. After reaching the maximum, the frequency of oscillation decreases with further increase in a , while the decay rate becomes nearly constant as the black hole approaches extremality. The decrease in the value of $-\text{Im}(\omega)$ with the tidal charge indicates that the $l = 0$ mode of the rotating braneworld black hole is more long-lived than its GR counterpart. Such a behavior has also been reported for gravitational perturbations in braneworld black holes [144].

From the top left panel of Fig. 2, we can also see that when the mass μ of scalar field is turned on, the modes move closer to the real axis. However, in the presence of μ , the change in the decay rate $\text{Im}(\omega)$ is much more pronounced than that in the frequency of oscillation $\text{Re}(\omega)$. In fact, if we keep β and a fixed, and gradually increase μ , then the imaginary part of the QNM will increasingly tend to a value very close to zero. Since these modes will have a finite $\text{Re}(\omega)$ and an extremely small but negative $\text{Im}(\omega)$, these modes will be arbitrarily long-lived. Such modes are called *quasiresonance modes* [89, 178, 190, 195–205] and they satisfy the QNM boundary conditions. They exist even for near extremal configurations and we explicitly demonstrate the same in Fig. 3.

The contour lines in the top panel of Fig. 4 indicate that the $l = m = 0$ modes with the largest oscillation frequency occur for smaller values of the tidal charge (that is, towards the left of the parameter space under consideration) and from the bottom panel of the same figure, we can see that these modes are also associated with a higher decay rate indicating that they are the least long-lived modes. We also see that the oscillation frequency is maximum when the two horizons of the BH are moderately separated but when the scalar field acquires mass, the maximum begins to shift towards extremal configurations. It is also evident from the bottom panel of Fig. 4 that the decay rate of perturbations in extremal configurations are smaller and hence they are more long-lived than their sub-extremal counterparts. Turning on μ , we can see (from scales on the colorbars) the corresponding decay rates become smaller. Lastly, we observe that the long-lived modes lie in the upper-right region of the parameter space for both the massless and massive cases, that is, in the regime of high values of both β and a , and the corresponding modes have the lowest frequency of oscillation.

Next we consider $l = 1$ modes, and we notice in Fig. 2 that the behavior of the modes varies with azimuthal

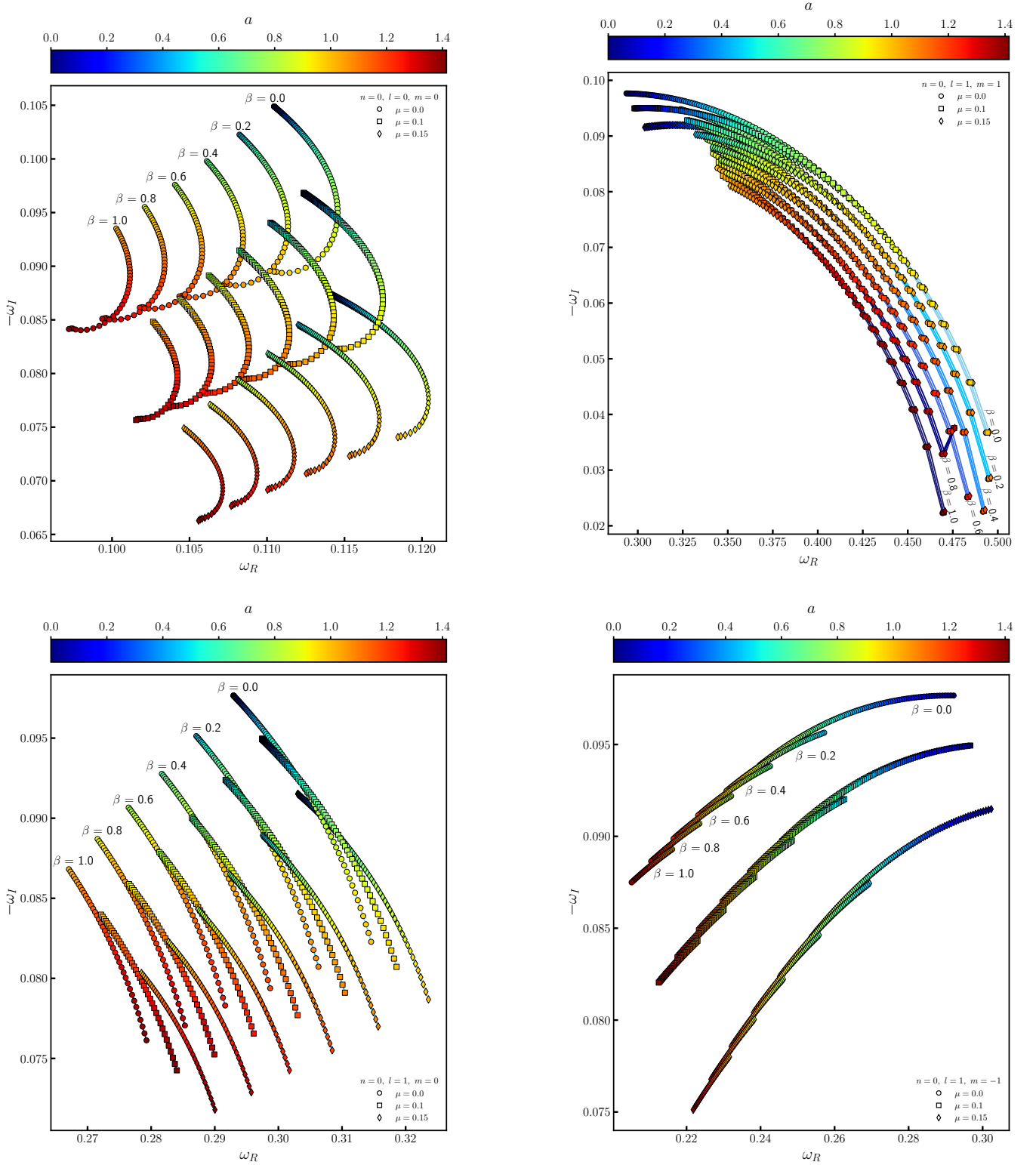


FIG. 2. The quasinormal mode spectra of the rotating braneworld black hole for $l = m = 0$ (top left), $l = m = 1$ (top right), $l = 1, m = 0$ (bottom left) and $l = 1, m = -1$ (bottom right). Each curve in the complex plane is labeled by β , and the color of each point corresponds to the value of a , whereas the value of μ is indicated by the shape of the marker. In this figures, the characteristic length scale given by M is set to unity.

number $m = -1, 0, 1$. However, in general, the introduction of tidal charge β leads to a decrease in the frequency

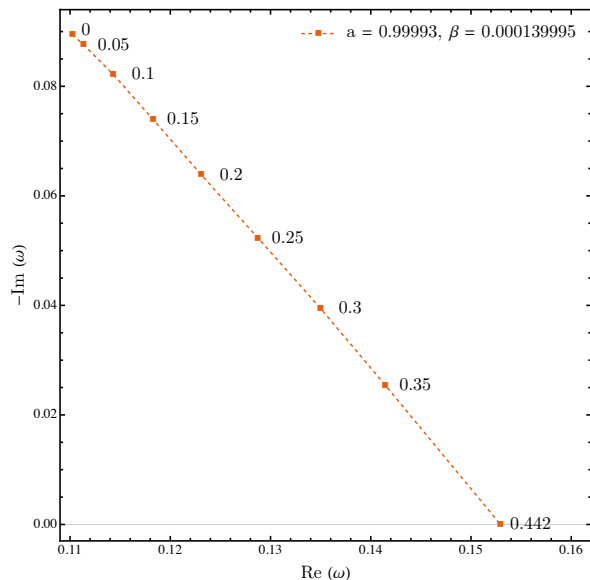


FIG. 3. The formation of quaresonance state in a near-extremal rotating braneworld black hole spacetime for $l = m = 0$ and $a \sim 1$ with $\beta > 0$. The labels alongside the points indicate the value of the scalar field mass.

of oscillation and the decay rate here as well since the curves labeled by $\beta > 0$ shifts towards the origin as β increases. It evident from Fig. 2 that all the $l = 1$ modes have a higher frequency of oscillation compared to the $l = 0$ modes for all the β and a values that have been considered. Notice that for the $m = 0, 1$ modes (bottom left and top right panels respectively), if we keep β fixed and increase a , then the frequency of oscillation increases whereas for $m = -1$ modes (bottom right panel), it decreases. The decay rates for all m values decrease if a is increased while keeping β fixed.

Let us first look closely at the $l = 1, m = -1$ modes: in the extreme left panel of Fig. 5, we see the modes with the smallest frequency of frequency of oscillation occur for larger values of both β and a as they tend to cluster on the upper right side of the parameter space, and from Fig. 6, it is evident that these modes also have smallest decay rates; the longest-lived modes therefore occur for smaller values β and a . The inclusion of μ does not change the qualitative behaviour of the modes even though they tend to reduce the values of both the oscillation frequency and decay rate. In fact, from the bottom right panel of Fig. 2, it clear that the change in the decay rate is much more drastic in the presence of μ compared to the change in the oscillation frequency. Moreover, for sufficiently large values of β and μ one could possibly obtain quaresonance modes near extremality.

Now, based on the middle panels Fig. 5 and Fig. 6, we observed that the $l = 1, m = 0$ modes with the smallest frequency of oscillation occurs for large values of β but smaller values a . But the near-extremal modes (especially those occurring near the top right corner of the parameter space) are the ones with the smallest decay

rates, and hence they are they are longest-lived modes. The aforementioned figures along with the bottom left panel of Fig. 2 also show that the presence of the mass μ increases the oscillation frequency of these modes but at the same time makes the modes long-lived by significantly decreasing the decay rate. In fact, for large enough values of β and μ , quaresonance could be achieved by these modes as well.

Let us finally talk about the $l = m = 1$ modes in detail: from the extreme right panel of Fig. 5, we see that oscillation frequencies of both massless and massive perturbations are higher for black holes near extremality, and since the contours are nearly parallel to the extremal curve, it indicates that they approach a constant value. The smallest values of both a and β corresponds to modes with the smallest oscillation frequencies. When it comes to the decay rates, from the extreme right panel of Fig. 6, it is clear that the near-extremal modes have the smallest decay rates and hence they are extremely long lived. In fact, for massless perturbations, they may be extremely close to zero. This feature can also be extrapolated from the trajectories in the complex plane as shown in the top right panel of Fig. 2, and it points towards the existence of the well known zero damped modes (ZDMs) [206, 207]. The ZDMs of near extreme and extreme Kerr and KN family of BHs have been extensively studied in the past, and they are quite distinct from the phenomenon of quaresonance mentioned earlier. The quaresonance modes are arbitrarily long lived and have a very small imaginary part: they are associated only with the presence of massive fields whereas ZDMs can occur only for certain values of m for massless perturbations. Now the mass of the scalar field has an intriguing effect on the behaviour of the modes: from Fig. 2 we see that for smaller values of β and a , increasing μ enhances the oscillation frequency slightly and reduces the decay rate but the effect is completely washed out as one approaches extremality. Notice how the modes corresponding to different values of μ clump together as one increases a while keeping β fixed in the top right panel of Fig. 2. It seems likely that near extremality, the quaresonance frequencies approach those of of the ZDMs. However, the interplay between ZDMs and quaresonance modes needs to be probed further numerically to arrive at a definite conclusion. We wish to return to such questions in the future.

Lastly, we end this section with the note that we could not to find any mode with $\text{Im}(\omega) > 0$ (in the region of the parameter space explored in this work) which points toward the stability of the rotating braneworld black hole as far as QNMs are concerned.

B. Superradiant instability

We now focus on the effect of the tidal charge on the quasibound states (QBSs) and the associated superradiant instability. For (massive) scalar fields around the

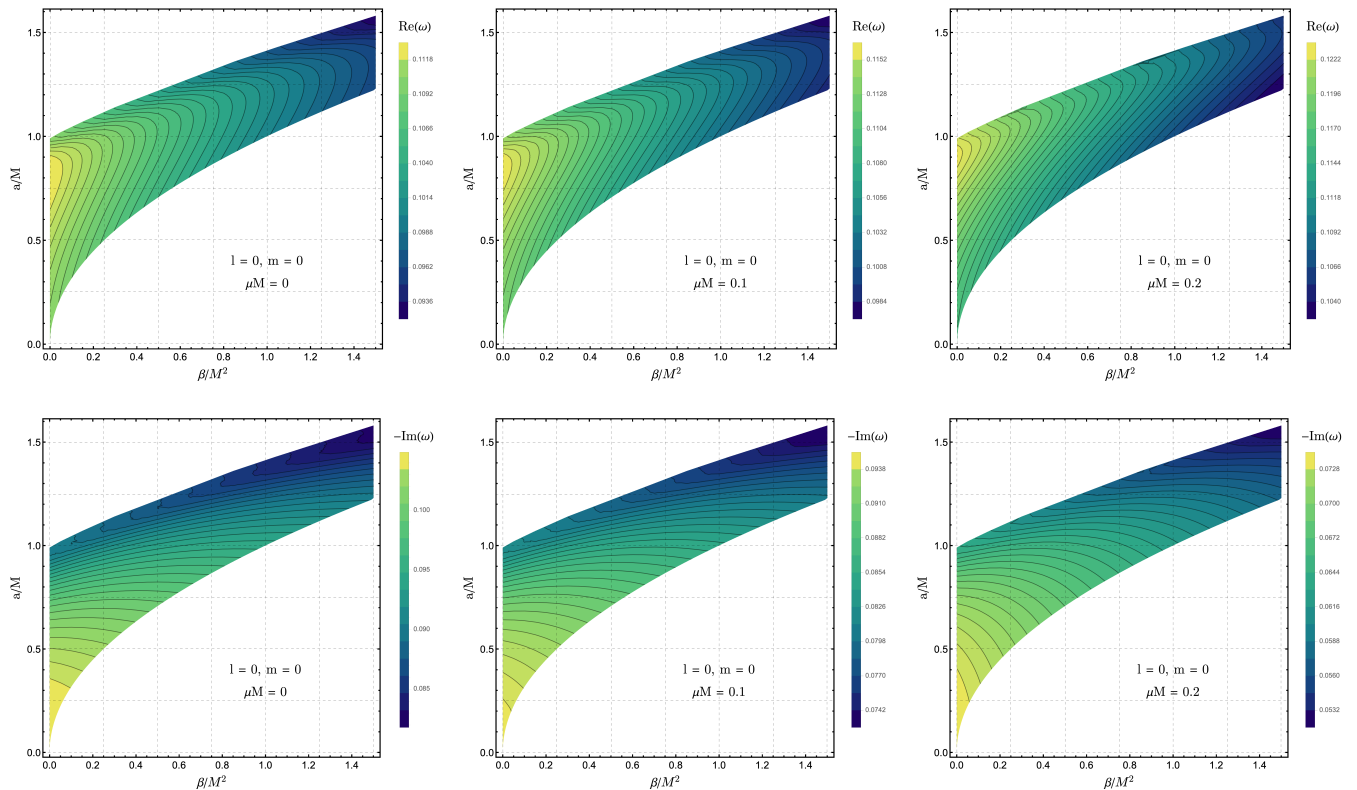


FIG. 4. The real (top row) and imaginary (bottom row) parts of the scalar quasinormal mode spectra corresponding to $l = m = 0$ for $\mu = 0$ (left column), $\mu = 0.1$ (middle column), $\mu = 0.2$ for the allowed values of a and β . The black holes M is set to unity.

Kerr BH, the most unstable modes are those corresponding to $l = m = 1$ and $n = 0$ [178]. Furthermore, taking a hint from the rich structure of the QBS spectrum of the KN black hole [184], we shall also restrict ourselves to the $l = m = 1$ and $n = 0$ modes.

First let us focus on the case when $a/M < 1$. The results are summarised in Fig. 7 where we have considered three values of the rotation parameter, $a = 0.9M, 0.99M, 0.997M$. For each value of a we have considered a set of values of tidal charge β normalized by the absolute minimum value of β , that is, $\beta_0/M^2 = |(a/M)^2 - 1|$ (c.f.:(2.4)) in order to aid comparison across the a values. Furthermore, the dashed curves in Fig. 7 correspond to $\beta < 0$ which are operationally similar to the KN case discussed in [184], and the solid curves correspond to $\beta > 0$. The solid black curve indicates to the Kerr case ($\beta = 0$). In general, $\text{Im}(\omega)$ increases with the mass μ of the scalar field and becomes positive. It then reaches a maximum value⁴ for some value of μ and on reaching this maximum, it decreases further with in-

creasing μ and eventually becomes negative. In the mass range where $\text{Im}(\omega) > 0$, $\text{Re}(\omega) < \omega_c$. It is interesting to note from Fig. 7 that:

- for $a = 0.9M$ (left panel of Fig. 7), the presence of a relatively large positive tidal charge suppresses the superradiant instability by roughly two orders of magnitude. For $\beta = -0.99\beta_0$, (i.e., when the BH is near-extreme) we find the highest peak value of $\text{Im}(\omega M) = 1.03832 \times 10^{-7}$ at $\mu M = 0.446114$ whereas for $\beta = 0.99\beta_0$, we observe the smallest peak value $\text{Im}(\omega M) = 4.5619 \times 10^{-9}$ at $\mu M = 0.243645$. Note that for $\beta = 0$, we find a peak value of $\text{Im}(\omega M) = 1.55244 \times 10^{-8}$ at $\mu M = 0.293274$.
- for $a = 0.99M$ (middle panel of Fig. 7), we observe that the peak of the instability does not vary monotonically with β [184] and the peak occurs for a negative value of the tidal charge (corresponding to a sub-extreme configuration, in contrast to the previous case). The presence of a positive tidal charge is unable to significantly suppress the superradiant instability. For $\beta = -0.8\beta_0$, we find the highest peak value of $\text{Im}(\omega M) = 1.64681 \times 10^{-7}$ at $\mu M = 0.452859$ whereas for $\beta = 0.99\beta_0$, we find the smallest peak value $\text{Im}(\omega M) = 1.16555 \times 10^{-7}$ at $\mu M = 0.393733$. Note that for $\beta = 0$, we

⁴ We can find the maximum of the curve by constructing an interpolating function using the data generated by the continued fraction method. The function can then be maximized using standard techniques.

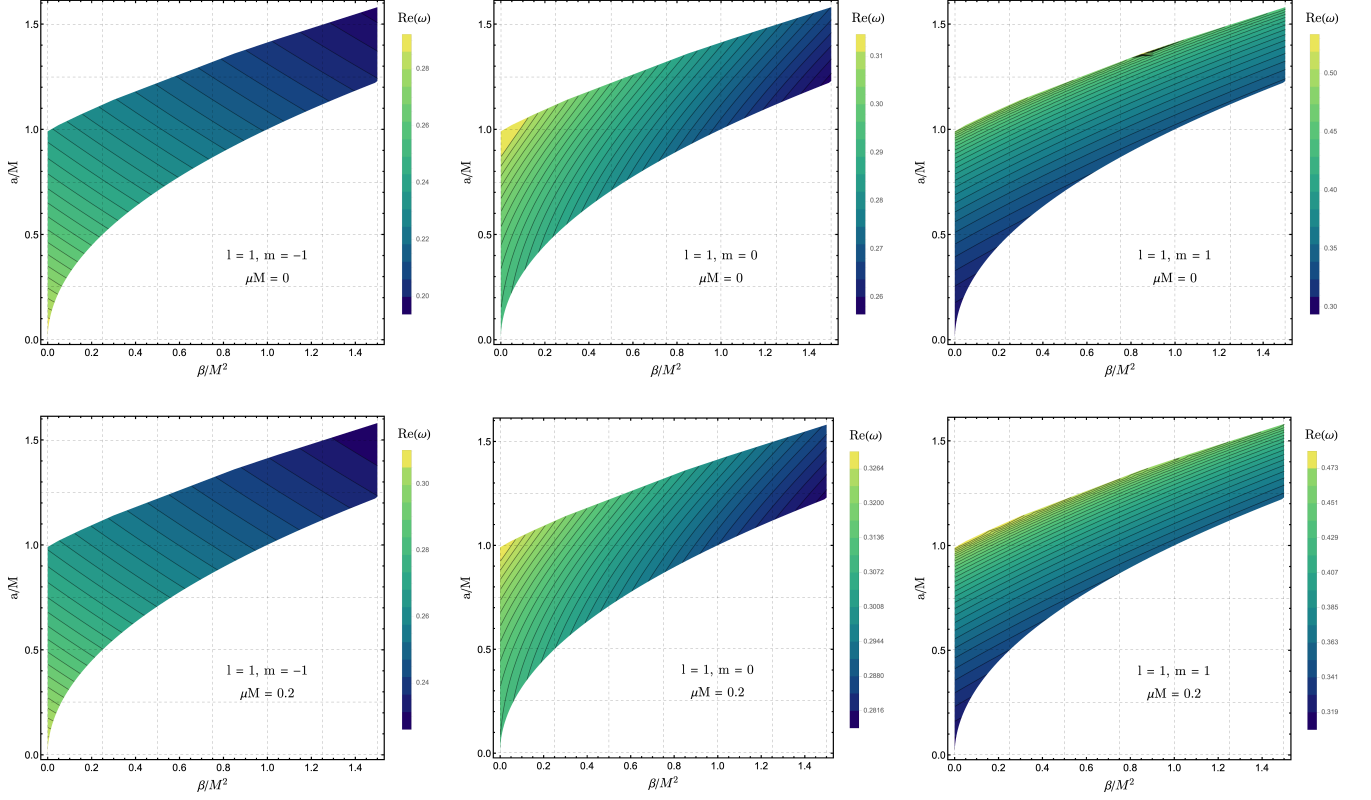


FIG. 5. The real part of the scalar quasinormal mode spectra corresponding to $l = 1$ and $m = -1$ (left column), $m = 0$ (middle column), $m = 1$ for the allowed values of a and β . The black holes M is set to unity for $\mu = 0$ (top row) and $\mu = 0.2$ bottom row. The black hole mass has been set to unity.

find a peak value of $\text{Im}(\omega M) = 1.50435 \times 10^{-7}$ at $\mu M = 0.42082$. These results are consistent with [184].

- for $a = 0.997M$ (right panel of Fig. 7), we obtain the maximum instability of $\text{Im}(\omega M) = 1.72275 \times 10^{-7}$ for $\beta = 0$ at $\mu M = 0.450511$ which is again consistent with [184]. Interestingly enough, now the smallest positive value of β that we had considered has a higher peak than all the negative values of β . Note that for $\beta = 0.8\beta_0$, we find the peak value of $\text{Im}(\omega M) = 1.70475 \times 10^{-7}$ at $\mu M = 0.439384$ whereas for $\beta = -0.99\beta_0$, we find the smallest peak value $\text{Im}(\omega M) = 1.60246 \times 10^{-7}$ at $\mu M = 0.449493$.
- If one were to solely focus on the positive values of the tidal charge, i.e., $\beta > 0$ but $a/M < 1$, it is clear from the three insets in Fig. 7, that decreasing β enhances the superradiant instability, and the corresponding peak values also increases with increase in a . But they always remain smaller than the corresponding peak values for $\beta = 0$. This appears to be consistent with the findings of [143] where the author studied the superradiant instability by examining the amplification factors of massless scalar

fields scattered by a rotating braneworld BH.

Let us now talk about the case when $a/M = 1$. The results are visualized in Fig. 8. In this case, the value of $\beta_0 = 0$ corresponds to the extreme Kerr BH. So we take a few representative values of $\beta/M^2 > 0$ to study the superradiant instability and do not normalize the value of β . We do not study the $\beta = 0, a = 1$ case because our numerical method is not equipped to handle extreme BHs. To study extreme BHs, the approach in [208] might be useful. We notice that moderate values tidal charge (that is, sub-extremal configurations) are able to significantly suppress the instability whereas the instability is enhanced in the presence of small positive values tidal charges. But intriguingly, the maximum instability *does not occur* for the smallest value of β considered. The maximum instability of $\text{Im}(\omega M) = 1.6912 \times 10^{-7}$ occurs for $\beta = 0.003M^2$ at $\mu M = 0.45278$ and we get the smallest peak value of $\text{Im}(\omega M) = 1.57103 \times 10^{-9}$ for $\beta = 0.8M^2$ at $\mu M = 0.202154$. Note that for $\beta = 0.001M^2$, the peak value is $\text{Im}(\omega M) = 1.64362 \times 10^{-7}$ at $\mu M = 0.45062$.

We now come to the case when $a > 1$. In Fig. 9, we consider three values of $a = 1.002M, 1.02M, 1.2M$ and suitably normalised values of the tidal charge $\beta/M^2 > 0$ as earlier. We summarize our findings below:

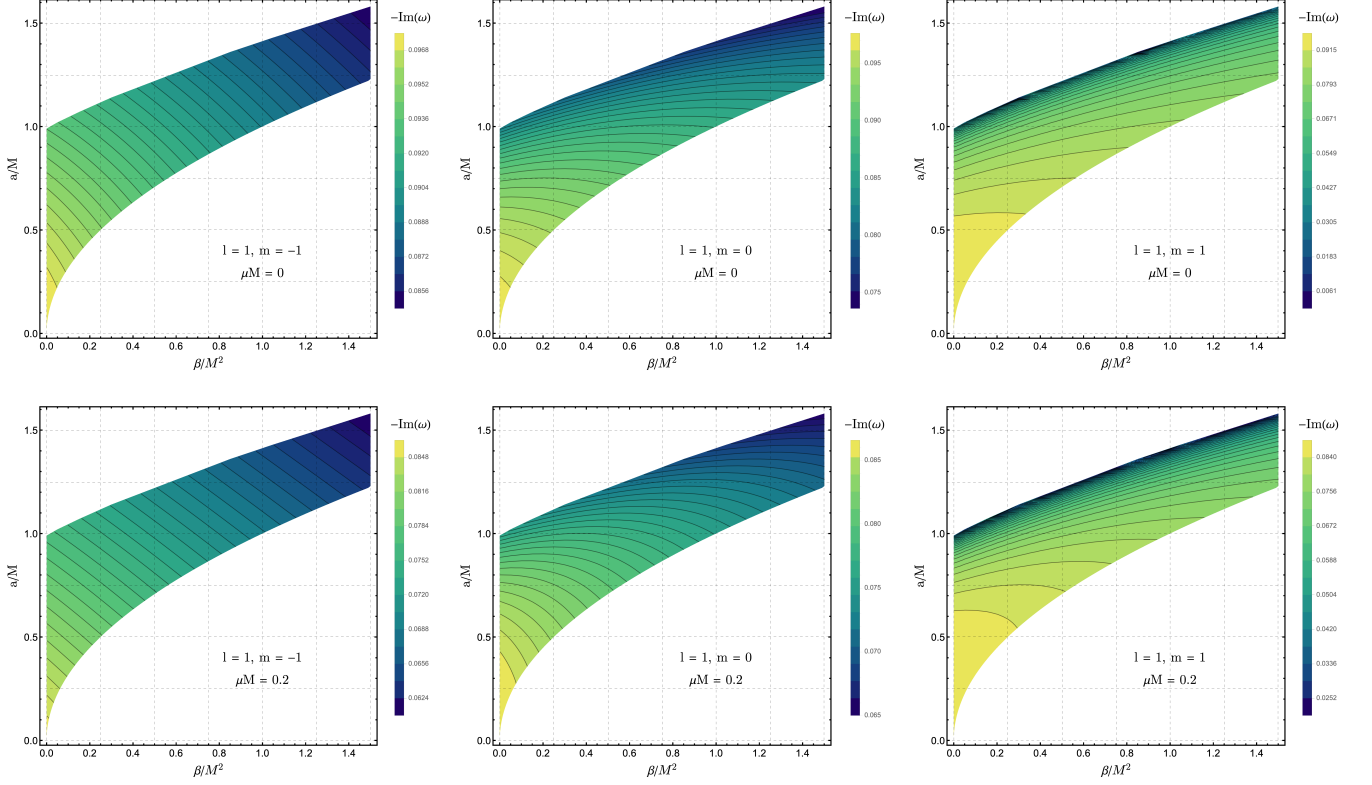


FIG. 6. The imaginary part of the scalar quasinormal mode spectra corresponding to $l = 1$ and $m = -1$ (left column), $m = 0$ (middle column), $m = 1$ for the allowed values of a and β . The black holes M is set to unity for $\mu = 0$ (top row) and $\mu = 0.2$ bottom row. The black hole mass has been set to unity.

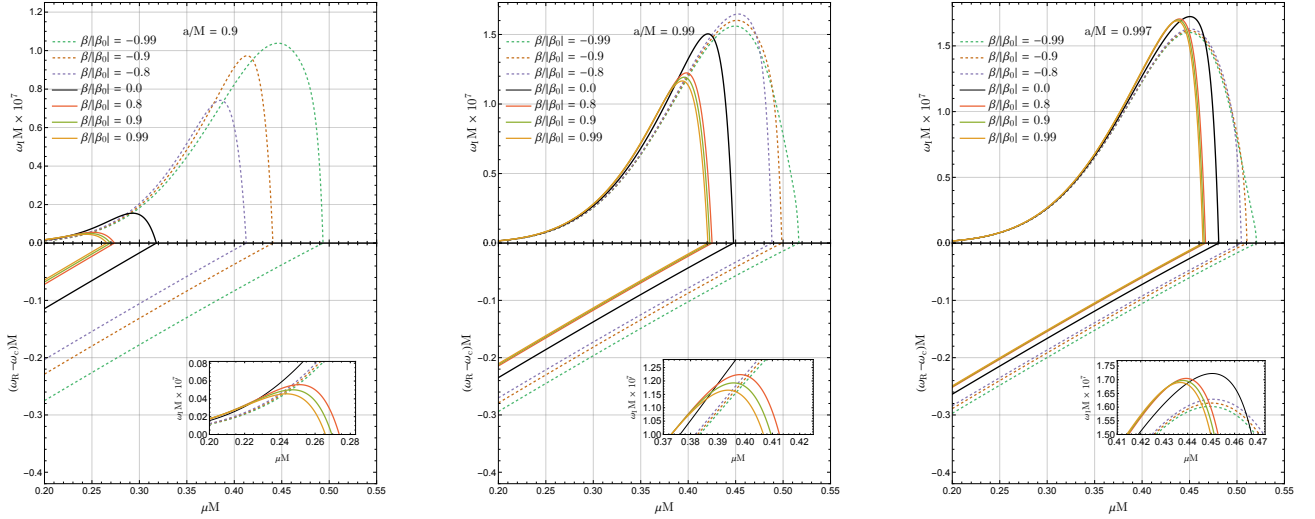


FIG. 7. The quasinbound state spectrum of a massive neutral scalar field ($l = m = 1$) for different values of BH spin $a < 1$ and tidal charge β .

- for $a = 1.002$ (left panel of Fig. 9), the value of the peak of the instability increases with increasing the tidal charge. In particular, the maximum

value of the peak $\text{Im}(\omega M) = 1.7595 \times 10^{-7}$ occurs for $\beta = 2.6\beta_0$ at $\mu M = 0.449823$. Note that for the instability is the least for $\beta = 1.05\beta_0$

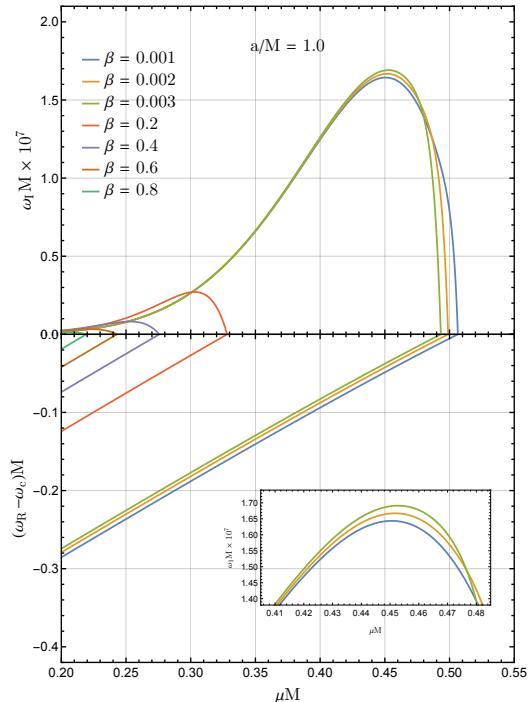


FIG. 8. The quasibound state spectrum of a massive neutral scalar field ($l = m = 1$) for $a = 1$ and different values of the tidal charge β .

with a peak value of $\text{Im}(\omega M) = 1.63817 \times 10^{-7}$ at $\mu M = 0.449787$.

- for $a = 1.02$ (middle panel of Fig. 9), we again see that the peak of the instability does not vary monotonically with β . The maximum peak occurs for an intermediate value of $\beta = 1.15\beta_0$ at $\text{Im}(\omega M) = 1.87952 \times 10^{-7}$ for $\mu M = 0.451168$.
- for $a = 1.2$ (right panel of Fig. 9), we notice a behaviour opposite to the one encountered for $a = 1.002$. We now see that increasing the tidal charge suppresses the superradiant instability by roughly a couple of orders of magnitude. For $\beta = 1.05\beta_0$, we find the highest peak value of $\text{Im}(\omega M) = 2.8151 \times 10^{-7}$ at $\mu M = 0.423676$ whereas for $\beta = 2.6\beta_0$, we observe the smallest peak value $\text{Im}(\omega M) = 7.17095 \times 10^{-9}$ at $\mu M = 0.230162$.
- if we focus on $\beta = 1.05\beta_0$ which by design corresponds to a near-extreme BH for all the three values of a that we have considered, we see from the insets in Fig. 9 that the superradiant instability for near-extreme BHs with $a > 1$ intensifies with increase in the value of a (and also the bare value of the tidal charge β). Looking at the same for

$\beta = 2.6\beta_0$, the opposite conclusion holds for sub-extremal braneworld black holes.

Lastly, in Fig. 10 we keep the tidal charge fixed at $\beta = 0.5M^2$, and study the superradiant instability by varying a whose values are normalized with respect to $a_{\text{max}}/M = \sqrt{1 + \beta/M^2}$. We note that the superradiant instability intensifies as a increases. In particular, the maximum value of the peak is $\text{Im}(\omega M) = 3.12115 \times 10^{-7}$ at $\mu M = 0.438173$ for a near-extreme BH with $a = 1.21974M^2$, or $a = 0.995918a_{\text{max}}$.

We summarize our results for the maximum peak of the superradiant instability for various values of a and β in Table I.

TABLE I. Maximum Peaks of Superradiant Instability

a/M	β/M^2	μM	$\text{Im}(\omega M)$
0.9	-0.1881000	0.446114	1.03832×10^{-7}
0.99	-0.0159200	0.452859	1.64681×10^{-7}
0.997	0	0.450511	1.72275×10^{-7}
1.0	0.003	0.45278	1.6912×10^{-7}
1.002	0.0104104	0.449823	1.7595×10^{-7}
1.02	0.0464600	0.451168	1.87952×10^{-7}
1.2	0.4620000	0.423676	2.8151×10^{-7}
1.21974	0.5	0.438173	3.12115×10^{-7}

We end this section with a few comments: Firstly we note that all of our figures clearly show that instability $\text{Im}(\omega) > 0$ always occurs in the superradiant regime, $0 < \text{Re}(\omega) < \omega_c$. Secondly, it is in general very difficult to estimate for what values of a, β, μ , the superradiant instability will be maximum. However, we may conclude that i) for $\beta > 0$ and $a < 1$, a higher value of the tidal charge would dampen the instability, ii) for $\beta > 0$ and $a \geq 1$, the maximum superradiant instability does not vary monotonically with β . The behaviour is highly nontrivial, especially when one compares it to results reported previously for massless scalar fields [143].

VI. FINAL REMARKS

The RS II rotating braneworld black hole solution provides us with a springboard to test the presence of an extra noncompact spatial dimension on gravitational interactions in the strong field regime. In this study, we have focused on the behaviour of a massive scalar field with $\mu M < 1$ propagating in the said black hole spacetime. Since the braneworld BH can be superspinning, we have focused on the region of the parameter space where $a > 1$ and $\beta > 0$. First we have made an in-depth study of the quasinormal mode spectra of massive scalar perturbations. Our analysis reveals that in the presence of the tidal charge β (which carries the imprint of the extra dimension) and scalar field mass μ , the modes are

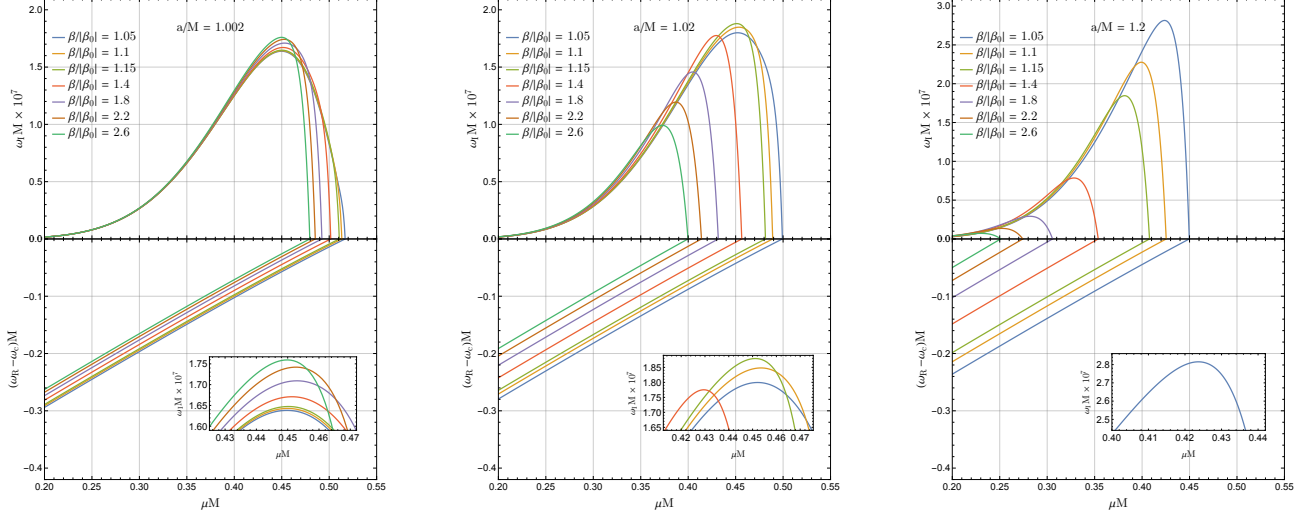


FIG. 9. The quasi-bound state spectrum of a massive neutral scalar field ($l = m = 1$) for different values of BH spin $a > 1$ and tidal charge β .

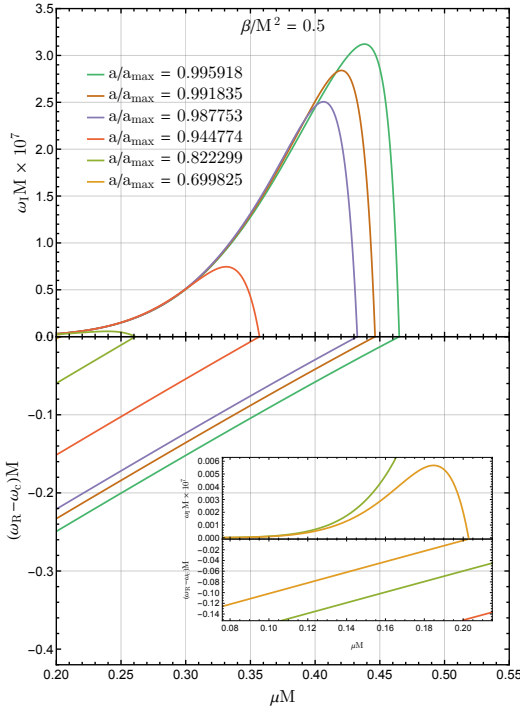


FIG. 10. The quasi-bound state spectrum of a neutral scalar field ($l = m = 1$) for different values of BH spin $a > 1$ and fixed tidal charge β .

long lived compared to the Kerr black hole. We have also noted the intricate behaviour shown by the modes cor-

responding to different values of the azimuthal number m for $l = 1$. We have further explored the formation of quairesonance modes and discussed the existence of zero damped modes as well.

Next, we have studied the superradiant instability associated with the spectra of the quasibound states, that is, the formation of the so-called gravitational atom. Our analysis reveals a highly non-trivial dependence of the peak of the superradiant instability on the tidal charge and the angular momentum of the black hole. For $a < 1$, the presence of the tidal charge always dampens the superradiant instability when one compares it to that of the Kerr BH. However, the dynamics is much richer when one looks at superspinning ($a > 1$) configurations. Notably, for such near extremal BHs, the superradiant instability intensifies with the tidal charge. These findings could have implications for ongoing efforts to detect boson clouds around black holes in order to constrain the mass of ultra light particles [164, 165, 169].

The present work offers numerous extensions. Some of us are attempting to investigate the phenomena of eigenvalue repulsions [209, 210] in the quasinormal mode spectra of the rotating braneworld black hole. Moreover, it has been pointed out that the QNM spectrum of black holes may be unstable against small perturbations to the scattering potential [194, 211]. It would be worthwhile to study the effect of the tidal charge on the instability of the QNM spectrum. One can also construct braneworld BH solutions that not asymptotically flat [212] and one may use these solutions to understand how the presence of both the cosmological constant and the extra dimension change the behaviour of the QNM spectrum. It would also be interesting to see how the presence of the tidal charge affects the superradiant in-

stability in the regime $\mu \sim \omega$ when the scalar field is charged following [182, 184]. Lastly, both scalar and vector boson clouds around Kerr BHs have attracted a lot of attention in recent years, especially in the context of gravitational wave astronomy with binary black holes and people have already explored various aspects of such gravitational atoms [165–168, 213–220]. It would be interesting to extend these studies to the braneworld scenario. Note that in [221], the superradiant instability and the formation of the vector gravitational atom was studied for the Kerr Newman black hole. Such a pioneering investigation was possible only after solving the difficult problem of separating the Proca equation by exploiting certain hidden symmetries of the spacetime. Our preliminary investigations indicate that many of these problems can be extended in to the braneworld scenario and the

presence of the tidal charge will leave a clear mark of the extra dimension on these systems. We wish to study some of these aspects in the future.

ACKNOWLEDGMENTS

S.S. acknowledges funding from SERB, DST, Government of India through the Core Research Grant CRG/2020/004347. A.A.S. acknowledges the funding from SERB, Govt. of India under the Core Research Grant CRG/2020/004347. S.S.B. acknowledges the funding from the University Grants Commission, Govt. of India under JRF scheme. The authors would like to thank Srijit Bhattacharjee, Sumanta Chakraborty and Mostafizur Rahman for useful discussions.

-
- [1] B. P. Abbott *et al.* (LIGO Scientific, Virgo), Observation of Gravitational Waves from a Binary Black Hole Merger, *Phys. Rev. Lett.* **116**, 061102 (2016), [arXiv:1602.03837 \[gr-qc\]](#).
 - [2] B. P. Abbott *et al.* (LIGO Scientific, Virgo), GW170817: Observation of Gravitational Waves from a Binary Neutron Star Inspiral, *Phys. Rev. Lett.* **119**, 161101 (2017), [arXiv:1710.05832 \[gr-qc\]](#).
 - [3] B. P. Abbott *et al.* (LIGO Scientific, Virgo), GWTC-1: A Gravitational-Wave Transient Catalog of Compact Binary Mergers Observed by LIGO and Virgo during the First and Second Observing Runs, *Phys. Rev. X* **9**, 031040 (2019), [arXiv:1811.12907 \[astro-ph.HE\]](#).
 - [4] K. Akiyama *et al.* (Event Horizon Telescope), First M87 Event Horizon Telescope Results. I. The Shadow of the Supermassive Black Hole, *Astrophys. J. Lett.* **875**, L1 (2019), [arXiv:1906.11238 \[astro-ph.GA\]](#).
 - [5] K. Akiyama *et al.* (Event Horizon Telescope), First M87 Event Horizon Telescope Results. IV. Imaging the Central Supermassive Black Hole, *Astrophys. J. Lett.* **875**, L4 (2019), [arXiv:1906.11241 \[astro-ph.GA\]](#).
 - [6] K. Akiyama *et al.* (Event Horizon Telescope), First M87 Event Horizon Telescope Results. VII. Polarization of the Ring, *Astrophys. J. Lett.* **910**, L12 (2021), [arXiv:2105.01169 \[astro-ph.HE\]](#).
 - [7] K. Akiyama *et al.* (Event Horizon Telescope), First M87 Event Horizon Telescope Results. VIII. Magnetic Field Structure near The Event Horizon, *Astrophys. J. Lett.* **910**, L13 (2021), [arXiv:2105.01173 \[astro-ph.HE\]](#).
 - [8] K. Akiyama *et al.* (Event Horizon Telescope), First M87 Event Horizon Telescope Results. IX. Detection of Near-horizon Circular Polarization, *Astrophys. J. Lett.* **957**, L20 (2023), [arXiv:2311.10976 \[astro-ph.HE\]](#).
 - [9] K. Akiyama *et al.* (Event Horizon Telescope), First Sagittarius A* Event Horizon Telescope Results. I. The Shadow of the Supermassive Black Hole in the Center of the Milky Way, *Astrophys. J. Lett.* **930**, L12 (2022), [arXiv:2311.08680 \[astro-ph.HE\]](#).
 - [10] K. Akiyama *et al.* (Event Horizon Telescope), First Sagittarius A* Event Horizon Telescope Results. III. Imaging of the Galactic Center Supermassive Black Hole, *Astrophys. J. Lett.* **930**, L14 (2022), [arXiv:2311.09479 \[astro-ph.HE\]](#).
 - [11] R. Abuter *et al.* (GRAVITY), Detection of the gravitational redshift in the orbit of the star S2 near the Galactic centre massive black hole, *Astron. Astrophys.* **615**, L15 (2018), [arXiv:1807.09409 \[astro-ph.GA\]](#).
 - [12] T. Do *et al.*, Relativistic redshift of the star S0-2 orbiting the Galactic center supermassive black hole, *Science* **365**, 664 (2019), [arXiv:1907.10731 \[astro-ph.GA\]](#).
 - [13] R. Abuter *et al.* (GRAVITY), Detection of the Schwarzschild precession in the orbit of the star S2 near the Galactic centre massive black hole, *Astron. Astrophys.* **636**, L5 (2020), [arXiv:2004.07187 \[astro-ph.GA\]](#).
 - [14] O. Dreyer, B. J. Kelly, B. Krishnan, L. S. Finn, D. Garrison, and R. Lopez-Aleman, Black hole spectroscopy: Testing general relativity through gravitational wave observations, *Class. Quant. Grav.* **21**, 787 (2004), [arXiv:gr-qc/0309007](#).
 - [15] E. Berti, K. Yagi, and N. Yunes, Extreme Gravity Tests with Gravitational Waves from Compact Binary Coalescences: (I) Inspiral-Merger, *Gen. Rel. Grav.* **50**, 46 (2018), [arXiv:1801.03208 \[gr-qc\]](#).
 - [16] E. Berti, K. Yagi, H. Yang, and N. Yunes, Extreme Gravity Tests with Gravitational Waves from Compact Binary Coalescences: (II) Ringdown, *Gen. Rel. Grav.* **50**, 49 (2018), [arXiv:1801.03587 \[gr-qc\]](#).
 - [17] K. Yagi and L. C. Stein, Black Hole Based Tests of General Relativity, *Class. Quant. Grav.* **33**, 054001 (2016), [arXiv:1602.02413 \[gr-qc\]](#).
 - [18] K. Hioki and K.-i. Maeda, Measurement of the Kerr Spin Parameter by Observation of a Compact Object's Shadow, *Phys. Rev. D* **80**, 024042 (2009), [arXiv:0904.3575 \[astro-ph.HE\]](#).
 - [19] C. Bambi, Can the supermassive objects at the centers of galaxies be traversable wormholes? The first test of strong gravity for mm/sub-mm very long baseline interferometry facilities, *Phys. Rev. D* **87**, 107501 (2013), [arXiv:1304.5691 \[gr-qc\]](#).
 - [20] C. Bambi, Testing black hole candidates with electromagnetic radiation, *Rev. Mod. Phys.* **89**, 025001 (2017), [arXiv:1509.03884 \[gr-qc\]](#).
 - [21] P. V. P. Cunha and C. A. R. Herdeiro, Shadows and strong gravitational lensing: a brief review, *Gen. Rel.*

- Grav.* **50**, 42 (2018), [arXiv:1801.00860 \[gr-qc\]](#).
- [22] R. Narayan, M. D. Johnson, and C. F. Gammie, The Shadow of a Spherically Accreting Black Hole, *Astrophys. J. Lett.* **885**, L33 (2019), [arXiv:1910.02957 \[astro-ph.HE\]](#).
- [23] S. E. Gralla, D. E. Holz, and R. M. Wald, Black Hole Shadows, Photon Rings, and Lensing Rings, *Phys. Rev. D* **100**, 024018 (2019), [arXiv:1906.00873 \[astro-ph.HE\]](#).
- [24] D. Psaltis *et al.* (Event Horizon Telescope), Gravitational Test Beyond the First Post-Newtonian Order with the Shadow of the M87 Black Hole, *Phys. Rev. Lett.* **125**, 141104 (2020), [arXiv:2010.01055 \[gr-qc\]](#).
- [25] C. Bambi, K. Freese, S. Vagnozzi, and L. Visinelli, Testing the rotational nature of the supermassive object M87* from the circularity and size of its first image, *Phys. Rev. D* **100**, 044057 (2019), [arXiv:1904.12983 \[gr-qc\]](#).
- [26] A. Amorim *et al.* (GRAVITY), Test of the Einstein Equivalence Principle near the Galactic Center Supermassive Black Hole, *Phys. Rev. Lett.* **122**, 101102 (2019), [arXiv:1902.04193 \[astro-ph.GA\]](#).
- [27] C. M. Will, Was Einstein right?: testing relativity at the centenary, *Annalen Phys.* **15**, 19 (2005), [arXiv:gr-qc/0504086](#).
- [28] C. M. Will, Resource Letter PTG-1: Precision Tests of Gravity, *Am. J. Phys.* **78**, 1240 (2010), [arXiv:1008.0296 \[gr-qc\]](#).
- [29] C. M. Will, The Confrontation between General Relativity and Experiment, *Living Rev. Rel.* **17**, 4 (2014), [arXiv:1403.7377 \[gr-qc\]](#).
- [30] C. M. Will, *Theory and Experiment in Gravitational Physics* (Cambridge University Press, 2018).
- [31] B. P. Abbott *et al.* (LIGO Scientific, Virgo), Properties of the Binary Black Hole Merger GW150914, *Phys. Rev. Lett.* **116**, 241102 (2016), [arXiv:1602.03840 \[gr-qc\]](#).
- [32] B. P. Abbott *et al.* (LIGO Scientific, Virgo), Tests of general relativity with GW150914, *Phys. Rev. Lett.* **116**, 221101 (2016), [Erratum: *Phys.Rev.Lett.* 121, 129902 (2018)], [arXiv:1602.03841 \[gr-qc\]](#).
- [33] B. P. Abbott *et al.* (LIGO Scientific, VIRGO), GW170104: Observation of a 50-Solar-Mass Binary Black Hole Coalescence at Redshift 0.2, *Phys. Rev. Lett.* **118**, 221101 (2017), [Erratum: *Phys.Rev.Lett.* 121, 129901 (2018)], [arXiv:1706.01812 \[gr-qc\]](#).
- [34] B. P. Abbott *et al.* (LIGO Scientific, Virgo), Tests of General Relativity with GW170817, *Phys. Rev. Lett.* **123**, 011102 (2019), [arXiv:1811.00364 \[gr-qc\]](#).
- [35] B. P. Abbott *et al.* (LIGO Scientific, Virgo), Tests of General Relativity with the Binary Black Hole Signals from the LIGO-Virgo Catalog GWTC-1, *Phys. Rev. D* **100**, 104036 (2019), [arXiv:1903.04467 \[gr-qc\]](#).
- [36] R. Abbott *et al.* (LIGO Scientific, Virgo), Tests of general relativity with binary black holes from the second LIGO-Virgo gravitational-wave transient catalog, *Phys. Rev. D* **103**, 122002 (2021), [arXiv:2010.14529 \[gr-qc\]](#).
- [37] R. Abbott *et al.* (LIGO Scientific, VIRGO, KAGRA), Tests of General Relativity with GWTC-3, (2021), [arXiv:2112.06861 \[gr-qc\]](#).
- [38] K. Akiyama *et al.* (Event Horizon Telescope), First M87 Event Horizon Telescope Results. VI. The Shadow and Mass of the Central Black Hole, *Astrophys. J. Lett.* **875**, L6 (2019), [arXiv:1906.11243 \[astro-ph.GA\]](#).
- [39] P. Kocherlakota *et al.* (Event Horizon Telescope), Constraints on black-hole charges with the 2017 EHT observations of M87*, *Phys. Rev. D* **103**, 104047 (2021), [arXiv:2105.09343 \[gr-qc\]](#).
- [40] K. Akiyama *et al.* (Event Horizon Telescope), First Sagittarius A* Event Horizon Telescope Results. VI. Testing the Black Hole Metric, *Astrophys. J. Lett.* **930**, L17 (2022), [arXiv:2311.09484 \[astro-ph.HE\]](#).
- [41] E. Berti, A. Buonanno, and C. M. Will, Estimating spinning binary parameters and testing alternative theories of gravity with LISA, *Phys. Rev. D* **71**, 084025 (2005), [arXiv:gr-qc/0411129](#).
- [42] V. Cardoso, L. Gualtieri, C. Herdeiro, and U. Sperhake, Exploring New Physics Frontiers Through Numerical Relativity, *Living Rev. Relativity* **18**, 1 (2015), [arXiv:1409.0014 \[gr-qc\]](#).
- [43] E. Berti *et al.*, Testing General Relativity with Present and Future Astrophysical Observations, *Class. Quant. Grav.* **32**, 243001 (2015), [arXiv:1501.07274 \[gr-qc\]](#).
- [44] L. Barack *et al.*, Black holes, gravitational waves and fundamental physics: a roadmap, *Class. Quant. Grav.* **36**, 143001 (2019), [arXiv:1806.05195 \[gr-qc\]](#).
- [45] N. Yunes and X. Siemens, Gravitational-Wave Tests of General Relativity with Ground-Based Detectors and Pulsar Timing-Arrays, *Living Rev. Rel.* **16**, 9 (2013), [arXiv:1304.3473 \[gr-qc\]](#).
- [46] E. Cannizzaro, G. Franciolini, and P. Pani, Novel tests of gravity using nano-Hertz stochastic gravitational-wave background signals, (2023), [arXiv:2307.11665 \[gr-qc\]](#).
- [47] P. Amaro-Seoane *et al.*, Low-frequency gravitational-wave science with eLISA/NGO, *Class. Quant. Grav.* **29**, 124016 (2012), [arXiv:1202.0839 \[gr-qc\]](#).
- [48] E. Berti *et al.*, Tests of General Relativity and Fundamental Physics with Space-based Gravitational Wave Detectors, (2019), [arXiv:1903.02781 \[astro-ph.HE\]](#).
- [49] E. Barausse *et al.*, Prospects for Fundamental Physics with LISA, *Gen. Rel. Grav.* **52**, 81 (2020), [arXiv:2001.09793 \[gr-qc\]](#).
- [50] K. G. Arun *et al.* (LISA), New horizons for fundamental physics with LISA, *Living Rev. Rel.* **25**, 4 (2022), [arXiv:2205.01597 \[gr-qc\]](#).
- [51] J. Luo *et al.* (TianQin), TianQin: a space-borne gravitational wave detector, *Class. Quant. Grav.* **33**, 035010 (2016), [arXiv:1512.02076 \[astro-ph.IM\]](#).
- [52] M. A. Abramowicz, W. Kluzniak, and J.-P. Lasota, No observational proof of the black hole event-horizon, *Astron. Astrophys.* **396**, L31 (2002), [arXiv:astro-ph/0207270](#).
- [53] V. Cardoso, E. Franzin, and P. Pani, Is the gravitational-wave ringdown a probe of the event horizon?, *Phys. Rev. Lett.* **116**, 171101 (2016), [Erratum: *Phys.Rev.Lett.* 117, 089902 (2016)], [arXiv:1602.07309 \[gr-qc\]](#).
- [54] V. Cardoso and P. Pani, Testing the nature of dark compact objects: a status report, *Living Rev. Rel.* **22**, 4 (2019), [arXiv:1904.05363 \[gr-qc\]](#).
- [55] Y. Mizuno, Z. Younsi, C. M. Fromm, O. Porth, M. De Laurentis, H. Olivares, H. Falcke, M. Kramer, and L. Rezzolla, The Current Ability to Test Theories of Gravity with Black Hole Shadows, *Nature Astron.* **2**, 585 (2018), [arXiv:1804.05812 \[astro-ph.GA\]](#).
- [56] S. E. Gralla, Can the EHT M87 results be used to test general relativity?, *Phys. Rev. D* **103**, 024023 (2021), [arXiv:2010.08557 \[astro-ph.HE\]](#).

- [57] R. Penrose, Gravitational collapse and space-time singularities, *Phys. Rev. Lett.* **14**, 57 (1965).
- [58] S. W. Hawking, Breakdown of Predictability in Gravitational Collapse, *Phys. Rev. D* **14**, 2460 (1976).
- [59] D. Christodoulou, The formation of black holes and singularities in spherically symmetric gravitational collapse, *Commun. Pure Appl. Math.* **44**, 339 (1991).
- [60] A. Ori, Inner structure of a charged black hole: An exact mass-inflation solution, *Phys. Rev. Lett.* **67**, 789 (1991).
- [61] M. Dafermos, The Interior of charged black holes and the problem of uniqueness in general relativity, *Commun. Pure Appl. Math.* **58**, 0445 (2005), [arXiv:gr-qc/0307013](#).
- [62] S. Bhattacharjee, S. Sarkar, and A. Virmani, Internal Structure of Charged AdS Black Holes, *Phys. Rev. D* **93**, 124029 (2016), [arXiv:1604.03730 \[hep-th\]](#).
- [63] V. Cardoso, J. a. L. Costa, K. Destounis, P. Hintz, and A. Jansen, Quasinormal modes and Strong Cosmic Censorship, *Phys. Rev. Lett.* **120**, 031103 (2018), [arXiv:1711.10502 \[gr-qc\]](#).
- [64] O. J. C. Dias, H. S. Reall, and J. E. Santos, The BTZ black hole violates strong cosmic censorship, *JHEP* **12**, 097, [arXiv:1906.08265 \[hep-th\]](#).
- [65] M. Rahman, On the validity of Strong Cosmic Censorship Conjecture in presence of Dirac fields, *Eur. Phys. J. C* **80**, 360 (2020), [arXiv:1905.06675 \[gr-qc\]](#).
- [66] M. Rahman, S. Mitra, and S. Chakraborty, Strong cosmic censorship conjecture with NUT charge and conformal coupling, *Class. Quant. Grav.* **37**, 195004 (2020), [arXiv:2001.00599 \[gr-qc\]](#).
- [67] M. Rahman, *Gravity in Modified Theories*, Ph.D. thesis, Jamia Milia Islamia University, Centre for Theoretical Physics, India (2020).
- [68] S. Bhattacharjee, S. Kumar, and S. Sarkar, Mass inflation and strong cosmic censorship in a nonextreme BTZ black hole, *Phys. Rev. D* **102**, 044030 (2020), [arXiv:2005.09705 \[gr-qc\]](#).
- [69] S. Bhattacharjee, S. Sarkar, and A. Bhattacharyya, Scalar perturbations of black holes in Jackiw-Teitelboim gravity, *Phys. Rev. D* **103**, 024008 (2021), [arXiv:2011.08179 \[gr-qc\]](#).
- [70] S. W. Hawking, Particle Creation by Black Holes, *Commun. Math. Phys.* **43**, 199 (1975), [Erratum: *Commun. Math. Phys.* **46**, 206 (1976)].
- [71] S. Chakraborty and K. Lochan, Black Holes: Eliminating Information or Illuminating New Physics?, *Universe* **3**, 55 (2017), [arXiv:1702.07487 \[gr-qc\]](#).
- [72] S. D. Mathur, The Information paradox: A Pedagogical introduction, *Class. Quant. Grav.* **26**, 224001 (2009), [arXiv:0909.1038 \[hep-th\]](#).
- [73] S. Perlmutter *et al.* (Supernova Cosmology Project), Measurements of Ω and Λ from 42 high redshift supernovae, *Astrophys. J.* **517**, 565 (1999), [arXiv:astro-ph/9812133](#).
- [74] A. G. Riess *et al.* (Supernova Search Team), Observational evidence from supernovae for an accelerating universe and a cosmological constant, *Astron. J.* **116**, 1009 (1998), [arXiv:astro-ph/9805201](#).
- [75] V. Sahni and A. A. Starobinsky, The Case for a positive cosmological Lambda term, *Int. J. Mod. Phys. D* **9**, 373 (2000), [arXiv:astro-ph/9904398](#).
- [76] T. Padmanabhan, Cosmological constant: The Weight of the vacuum, *Phys. Rept.* **380**, 235 (2003), [arXiv:hep-th/0212290](#).
- [77] P. J. E. Peebles and B. Ratra, The Cosmological Constant and Dark Energy, *Rev. Mod. Phys.* **75**, 559 (2003), [arXiv:astro-ph/0207347](#).
- [78] V. C. Rubin, W. K. Ford, Jr., and N. Thonnard, Extended rotation curves of high-luminosity spiral galaxies. IV. Systematic dynamical properties, Sa through Sc, *Astrophys. J. Lett.* **225**, L107 (1978).
- [79] G. Bertone and D. Hooper, History of dark matter, *Rev. Mod. Phys.* **90**, 045002 (2018), [arXiv:1605.04909 \[astro-ph.CO\]](#).
- [80] S. Nojiri and S. D. Odintsov, Introduction to modified gravity and gravitational alternative for dark energy, *eConf C0602061*, 06 (2006), [arXiv:hep-th/0601213](#).
- [81] T. Clifton, P. G. Ferreira, A. Padilla, and C. Skordis, Modified Gravity and Cosmology, *Phys. Rept.* **513**, 1 (2012), [arXiv:1106.2476 \[astro-ph.CO\]](#).
- [82] S. Nojiri, S. D. Odintsov, and V. K. Oikonomou, Modified Gravity Theories on a Nutshell: Inflation, Bounce and Late-time Evolution, *Phys. Rept.* **692**, 1 (2017), [arXiv:1705.11098 \[gr-qc\]](#).
- [83] S. Shankaranarayanan and J. P. Johnson, Modified theories of gravity: Why, how and what?, *Gen. Rel. Grav.* **54**, 44 (2022), [arXiv:2204.06533 \[gr-qc\]](#).
- [84] S. Nojiri and S. D. Odintsov, Unified cosmic history in modified gravity: from F(R) theory to Lorentz non-invariant models, *Phys. Rept.* **505**, 59 (2011), [arXiv:1011.0544 \[gr-qc\]](#).
- [85] A. De Felice and S. Tsujikawa, f(R) theories, *Living Rev. Rel.* **13**, 3 (2010), [arXiv:1002.4928 \[gr-qc\]](#).
- [86] T. Padmanabhan and D. Kothawala, Lanczos-Lovelock models of gravity, *Phys. Rept.* **531**, 115 (2013), [arXiv:1302.2151 \[gr-qc\]](#).
- [87] S. F. Hassan and R. A. Rosen, Bimetric Gravity from Ghost-free Massive Gravity, *JHEP* **02**, 126, [arXiv:1109.3515 \[hep-th\]](#).
- [88] E. Babichev and M. Crisostomi, Restoring general relativity in massive bigravity theory, *Phys. Rev. D* **88**, 084002 (2013), [arXiv:1307.3640 \[gr-qc\]](#).
- [89] M. Rahman, A. A. Sen, and S. S. Bohra, Traversable wormholes in bimetric gravity, *Phys. Rev. D* **108**, 104008 (2023), [arXiv:2305.13013 \[gr-qc\]](#).
- [90] G. W. Horndeski, Second-order scalar-tensor field equations in a four-dimensional space, *Int. J. Theor. Phys.* **10**, 363 (1974).
- [91] T. P. Sotiriou and S.-Y. Zhou, Black hole hair in generalized scalar-tensor gravity, *Phys. Rev. Lett.* **112**, 251102 (2014), [arXiv:1312.3622 \[gr-qc\]](#).
- [92] E. Babichev, C. Charmousis, and A. Lehébel, Black holes and stars in Horndeski theory, *Class. Quant. Grav.* **33**, 154002 (2016), [arXiv:1604.06402 \[gr-qc\]](#).
- [93] L. Heisenberg, Generalization of the Proca Action, *JCAP* **05**, 015, [arXiv:1402.7026 \[hep-th\]](#).
- [94] A. De Felice, L. Heisenberg, R. Kase, S. Tsujikawa, Y.-l. Zhang, and G.-B. Zhao, Screening fifth forces in generalized Proca theories, *Phys. Rev. D* **93**, 104016 (2016), [arXiv:1602.00371 \[gr-qc\]](#).
- [95] M. Rahman and A. A. Sen, Astrophysical Signatures of Black holes in Generalized Proca Theories, *Phys. Rev. D* **99**, 024052 (2019), [arXiv:1810.09200 \[gr-qc\]](#).
- [96] J. M. Overduin and P. S. Wesson, Kaluza-Klein gravity, *Phys. Rept.* **283**, 303 (1997), [arXiv:gr-qc/9805018](#).
- [97] S. Raychaudhuri and K. Sridhar, *Particle Physics of Brane Worlds and Extra Dimensions*, Cambridge Monographs on Mathematical Physics (Cambridge Uni-

- versity Press, 2016).
- [98] L. Randall and R. Sundrum, A Large mass hierarchy from a small extra dimension, *Phys. Rev. Lett.* **83**, 3370 (1999), [arXiv:hep-ph/9905221](#).
- [99] L. Randall and R. Sundrum, An Alternative to compactification, *Phys. Rev. Lett.* **83**, 4690 (1999), [arXiv:hep-th/9906064](#).
- [100] A. Chamblin, S. W. Hawking, and H. S. Reall, Brane world black holes, *Phys. Rev. D* **61**, 065007 (2000), [arXiv:hep-th/9909205](#).
- [101] A. Chamblin, H. S. Reall, H.-a. Shinkai, and T. Shiromizu, Charged brane world black holes, *Phys. Rev. D* **63**, 064015 (2001), [arXiv:hep-th/0008177](#).
- [102] T. Shiromizu, K.-i. Maeda, and M. Sasaki, The Einstein equation on the 3-brane world, *Phys. Rev. D* **62**, 024012 (2000), [arXiv:gr-qc/9910076](#).
- [103] M. Sasaki, T. Shiromizu, and K.-i. Maeda, Gravity, stability and energy conservation on the Randall-Sundrum brane world, *Phys. Rev. D* **62**, 024008 (2000), [arXiv:hep-th/9912233](#).
- [104] T. Harko and M. K. Mak, Vacuum solutions of the gravitational field equations in the brane world model, *Phys. Rev. D* **69**, 064020 (2004), [arXiv:gr-qc/0401049](#).
- [105] A. N. Aliev and A. E. Gumrukcuoglu, Gravitational field equations on and off a 3-brane world, *Class. Quant. Grav.* **21**, 5081 (2004), [arXiv:hep-th/0407095](#).
- [106] J. Garriga and T. Tanaka, Gravity in the brane world, *Phys. Rev. Lett.* **84**, 2778 (2000), [arXiv:hep-th/9911055](#).
- [107] S. B. Giddings, E. Katz, and L. Randall, Linearized gravity in brane backgrounds, *JHEP* **03**, 023, [arXiv:hep-th/0002091](#).
- [108] R. Maartens, Cosmological dynamics on the brane, *Phys. Rev. D* **62**, 084023 (2000), [arXiv:hep-th/0004166](#).
- [109] R. Maartens, Geometry and dynamics of the brane world, in *Spanish Relativity Meeting on Reference Frames and Gravitomagnetism (EREs2000)* (2001) [arXiv:gr-qc/0101059](#).
- [110] N. Dadhich, R. Maartens, P. Papadopoulos, and V. Rezanian, Black holes on the brane, *Phys. Lett. B* **487**, 1 (2000), [arXiv:hep-th/0003061](#).
- [111] A. N. Aliev and A. E. Gumrukcuoglu, Charged rotating black holes on a 3-brane, *Phys. Rev. D* **71**, 104027 (2005), [arXiv:hep-th/0502223](#).
- [112] A. N. Aliev, Rotating Braneworld Black Holes, in *11th Marcel Grossmann Meeting on General Relativity* (2006) pp. 2830–2832, [arXiv:astro-ph/0612735](#).
- [113] A. N. Aliev and P. Talazan, Gravitational Effects of Rotating Braneworld Black Holes, *Phys. Rev. D* **80**, 044023 (2009), [arXiv:0906.1465 \[gr-qc\]](#).
- [114] A. N. Aliev, G. D. Esmer, and P. Talazan, Strong Gravity Effects of Rotating Black Holes: Quasiperiodic Oscillations, *Class. Quant. Grav.* **30**, 045010 (2013), [arXiv:1205.2838 \[gr-qc\]](#).
- [115] S. Bhattacharya, D. Choudhury, D. P. Jatkar, and A. A. Sen, Brane dynamics in the Randall-Sundrum model, inflation and graceful exit, *Class. Quant. Grav.* **19**, 5025 (2002), [arXiv:hep-th/0103248](#).
- [116] M. C. Bento, O. Bertolami, and A. A. Sen, Supergravity inflation on the brane, *Phys. Rev. D* **67**, 023504 (2003), [arXiv:gr-qc/0204046](#).
- [117] M. C. Bento, O. Bertolami, and A. A. Sen, Tachyonic inflation in the brane world scenario, *Phys. Rev. D* **67**, 063511 (2003), [arXiv:hep-th/0208124](#).
- [118] B. Mukhopadhyaya, S. Sen, and S. SenGupta, Does a Randall-Sundrum scenario create the illusion of a torsion free universe?, *Phys. Rev. Lett.* **89**, 121101 (2002), [Erratum: *Phys.Rev.Lett.* 89, 259902 (2002)], [arXiv:hep-th/0204242](#).
- [119] Y.-b. Kim, C. O. Lee, I.-b. Lee, and J.-J. Lee, Brane world of warp geometry: An Introductory review, *J. Korean Astron. Soc.* **37**, 1 (2004), [arXiv:hep-th/0307023](#).
- [120] P. Kanti, Black holes in theories with large extra dimensions: A Review, *Int. J. Mod. Phys. A* **19**, 4899 (2004), [arXiv:hep-ph/0402168](#).
- [121] A. Perez-Lorenzana, An Introduction to extra dimensions, *J. Phys. Conf. Ser.* **18**, 224 (2005), [arXiv:hep-ph/0503177](#).
- [122] R. Maartens and K. Koyama, Brane-World Gravity, *Living Rev. Rel.* **13**, 5 (2010), [arXiv:1004.3962 \[hep-th\]](#).
- [123] T. Adamo and E. T. Newman, The Kerr-Newman metric: A Review, *Scholarpedia* **9**, 31791 (2014), [arXiv:1410.6626 \[gr-qc\]](#).
- [124] D. J. H. Chung, L. L. Everett, and H. Davoudiasl, Experimental probes of the Randall-Sundrum infinite extra dimension, *Phys. Rev. D* **64**, 065002 (2001), [arXiv:hep-ph/0010103](#).
- [125] A. Y. Bin-Nun, Relativistic Images in Randall-Sundrum II Braneworld Lensing, *Phys. Rev. D* **81**, 123011 (2010), [arXiv:0912.2081 \[gr-qc\]](#).
- [126] A. Y. Bin-Nun, Lensing By Sgr A* as a Probe of Modified Gravity, *Phys. Rev. D* **82**, 064009 (2010), [arXiv:1004.0379 \[gr-qc\]](#).
- [127] L. Amarilla and E. F. Eiroa, Shadow of a rotating braneworld black hole, *Phys. Rev. D* **85**, 064019 (2012), [arXiv:1112.6349 \[gr-qc\]](#).
- [128] I. Banerjee, S. Chakraborty, and S. SenGupta, Silhouette of M87*: A New Window to Peek into the World of Hidden Dimensions, *Phys. Rev. D* **101**, 041301 (2020), [arXiv:1909.09385 \[gr-qc\]](#).
- [129] I. Banerjee, S. Chakraborty, and S. SenGupta, Decoding signatures of extra dimensions and estimating spin of quasars from the continuum spectrum, *Phys. Rev. D* **100**, 044045 (2019), [arXiv:1905.08043 \[gr-qc\]](#).
- [130] S. Vagnozzi and L. Visinelli, Hunting for extra dimensions in the shadow of M87*, *Phys. Rev. D* **100**, 024020 (2019), [arXiv:1905.12421 \[gr-qc\]](#).
- [131] J. C. S. Neves, Constraining the tidal charge of brane black holes using their shadows, *Eur. Phys. J. C* **80**, 717 (2020), [arXiv:2005.00483 \[gr-qc\]](#).
- [132] I. Banerjee, S. Chakraborty, and S. SenGupta, Hunting extra dimensions in the shadow of Sgr A*, *Phys. Rev. D* **106**, 084051 (2022), [arXiv:2207.09003 \[gr-qc\]](#).
- [133] J.-y. Shen, B. Wang, and R.-K. Su, The Signals from the brane-world black Hole, *Phys. Rev. D* **74**, 044036 (2006), [arXiv:hep-th/0607034](#).
- [134] B. Toshmatov, Z. Stuchlík, J. Schee, and B. Ahmedov, Quasinormal frequencies of black hole in the braneworld, *Phys. Rev. D* **93**, 124017 (2016), [arXiv:1605.02058 \[gr-qc\]](#).
- [135] S. Chakraborty, K. Chakravarti, S. Bose, and S. SenGupta, Signatures of extra dimensions in gravitational waves from black hole quasinormal modes, *Phys. Rev. D* **97**, 104053 (2018), [arXiv:1710.05188 \[gr-qc\]](#).
- [136] L. Visinelli, N. Bolis, and S. Vagnozzi, Brane-world extra dimensions in light of GW170817, *Phys. Rev. D* **97**, 064039 (2018), [arXiv:1711.06628 \[gr-qc\]](#).

- [137] A. Chowdhury and N. Banerjee, Quasinormal modes of a charged spherical black hole with scalar hair for scalar and Dirac perturbations, *Eur. Phys. J. C* **78**, 594 (2018), [arXiv:1807.09559 \[gr-qc\]](#).
- [138] M. Rahman, S. Chakraborty, S. SenGupta, and A. A. Sen, Fate of Strong Cosmic Censorship Conjecture in Presence of Higher Spacetime Dimensions, *JHEP* **03**, 178, [arXiv:1811.08538 \[gr-qc\]](#).
- [139] R. Dey, S. Chakraborty, and N. Afshordi, Echoes from braneworld black holes, *Phys. Rev. D* **101**, 104014 (2020), [arXiv:2001.01301 \[gr-qc\]](#).
- [140] R. Dey, S. Biswas, and S. Chakraborty, Ergoregion instability and echoes for braneworld black holes: Scalar, electromagnetic, and gravitational perturbations, *Phys. Rev. D* **103**, 084019 (2021), [arXiv:2010.07966 \[gr-qc\]](#).
- [141] S. Chakraborty, E. Maggio, A. Mazumdar, and P. Pani, Implications of the quantum nature of the black hole horizon on the gravitational-wave ringdown, *Phys. Rev. D* **106**, 024041 (2022), [arXiv:2202.09111 \[gr-qc\]](#).
- [142] K. Chakravarti, S. Chakraborty, S. Bose, and S. SenGupta, Tidal Love numbers of black holes and neutron stars in the presence of higher dimensions: Implications of GW170817, *Phys. Rev. D* **99**, 024036 (2019), [arXiv:1811.11364 \[gr-qc\]](#).
- [143] E. S. de Oliveira, Tidal-charge effects on the superradiance of rotating black holes, *Eur. Phys. J. C* **80**, 1048 (2020), [arXiv:2004.10122 \[gr-qc\]](#).
- [144] A. K. Mishra, A. Ghosh, and S. Chakraborty, Constraining extra dimensions using observations of black hole quasi-normal modes, *Eur. Phys. J. C* **82**, 820 (2022), [arXiv:2106.05558 \[gr-qc\]](#).
- [145] M. Rahman, S. Kumar, and A. Bhattacharyya, Gravitational wave from extreme mass-ratio inspirals as a probe of extra dimensions, *JCAP* **01**, 046, [arXiv:2212.01404 \[gr-qc\]](#).
- [146] A. K. Mishra, G. Carullo, and S. Chakraborty, Bounds on tidal charges from gravitational-wave ringdown observations, (2023), [arXiv:2311.03556 \[gr-qc\]](#).
- [147] S. Biswas, Massive scalar perturbation of extremal rotating braneworld black hole: Superradiant stability analysis, *Phys. Lett. B* **820**, 136597 (2021), [arXiv:2106.13837 \[gr-qc\]](#).
- [148] S. Mukherjee and S. Chakraborty, Transition from inspiral to plunge for braneworld EMRI, *Class. Quant. Grav.* **40**, 145013 (2023), [arXiv:2212.07018 \[gr-qc\]](#).
- [149] A. Abdujabbarov and B. Ahmedov, Charged Particle Motion Around Rotating Black Hole in Braneworld Immersed in Magnetic Field, *Phys. Rev. D* **81**, 044022 (2010), [arXiv:0905.2730 \[gr-qc\]](#).
- [150] A. F. Zakharov, Constraints on tidal charge of the supermassive black hole at the Galactic Center with trajectories of bright stars, *Eur. Phys. J. C* **78**, 689 (2018), [arXiv:1804.10374 \[gr-qc\]](#).
- [151] H.-X. Zhang, C. Li, P.-Z. He, Q.-Q. Fan, and J.-B. Deng, Optical properties of a Brane-World black hole as photons couple to the Weyl tensor, *Eur. Phys. J. C* **80**, 461 (2020), [arXiv:1912.07068 \[gr-qc\]](#).
- [152] I. Banerjee, S. Chakraborty, and S. SenGupta, Looking for extra dimensions in the observed quasi-periodic oscillations of black holes, *JCAP* **09**, 037, [arXiv:2105.06636 \[gr-qc\]](#).
- [153] E. S. de Oliveira, Scalar scattering from charged black holes on the brane, *Class. Quant. Grav.* **35**, 065007 (2018), [arXiv:1706.07734 \[gr-qc\]](#).
- [154] E. S. de Oliveira, Scalar scattering from black holes with tidal charge, *Eur. Phys. J. C* **78**, 876 (2018), [arXiv:1805.04987 \[gr-qc\]](#).
- [155] E. S. de Oliveira, Electromagnetic absorption, emission and scattering spectra of black holes with tidal charge, *Eur. Phys. J. Plus* **135**, 880 (2020), [arXiv:1904.11612 \[gr-qc\]](#).
- [156] E. S. de Oliveira, Scalar absorption cross section of rotating black holes with tidal charge, *Phys. Rev. D* **104**, 124008 (2021), [arXiv:2008.04468 \[gr-qc\]](#).
- [157] C. V. Vishveshwara, Scattering of Gravitational Radiation by a Schwarzschild Black-hole, *Nature* **227**, 936 (1970).
- [158] E. Berti, V. Cardoso, and A. O. Starinets, Quasinormal modes of black holes and black branes, *Class. Quant. Grav.* **26**, 163001 (2009), [arXiv:0905.2975 \[gr-qc\]](#).
- [159] R. Konoplya and A. Zhidenko, Quasinormal modes of black holes: From astrophysics to string theory, *Rev. Mod. Phys.* **83**, 793 (2011), [arXiv:1102.4014 \[gr-qc\]](#).
- [160] R. Brito, V. Cardoso, and P. Pani, Superradiance: New Frontiers in Black Hole Physics, *Lect. Notes Phys.* **906**, pp.1 (2015), [arXiv:1501.06570 \[gr-qc\]](#).
- [161] W. H. Press and S. A. Teukolsky, Floating Orbits, Superradiant Scattering and the Black-hole Bomb, *Nature* **238**, 211 (1972).
- [162] V. Cardoso, O. J. C. Dias, J. P. S. Lemos, and S. Yoshida, The Black hole bomb and superradiant instabilities, *Phys. Rev. D* **70**, 044039 (2004), [Erratum: *Phys. Rev. D* **70**, 049903 (2004)], [arXiv:hep-th/0404096](#).
- [163] A. Arvanitaki, S. Dimopoulos, S. Dubovsky, N. Kaloper, and J. March-Russell, String Axiverse, *Phys. Rev. D* **81**, 123530 (2010), [arXiv:0905.4720 \[hep-th\]](#).
- [164] A. Arvanitaki and S. Dubovsky, Exploring the String Axiverse with Precision Black Hole Physics, *Phys. Rev. D* **83**, 044026 (2011), [arXiv:1004.3558 \[hep-th\]](#).
- [165] D. Baumann, H. S. Chia, and R. A. Porto, Probing Ultralight Bosons with Binary Black Holes, *Phys. Rev. D* **99**, 044001 (2019), [arXiv:1804.03208 \[gr-qc\]](#).
- [166] D. Baumann, H. S. Chia, R. A. Porto, and J. Stout, Gravitational Collider Physics, *Phys. Rev. D* **101**, 083019 (2020), [arXiv:1912.04932 \[gr-qc\]](#).
- [167] D. Baumann, H. S. Chia, J. Stout, and L. ter Haar, The Spectra of Gravitational Atoms, *JCAP* **12**, 006, [arXiv:1908.10370 \[gr-qc\]](#).
- [168] D. Baumann, G. Bertone, J. Stout, and G. M. Tomaselli, Ionization of gravitational atoms, *Phys. Rev. D* **105**, 115036 (2022), [arXiv:2112.14777 \[gr-qc\]](#).
- [169] A. Foschi *et al.* (GRAVITY), Using the motion of S2 to constrain scalar clouds around Sgr A*, *Mon. Not. Roy. Astron. Soc.* **524**, 1075 (2023), [arXiv:2306.17215 \[astro-ph.GA\]](#).
- [170] E. Cannizzaro, L. Sberna, S. R. Green, and S. Hollands, Relativistic perturbation theory for black-hole boson clouds, (2023), [arXiv:2309.10021 \[gr-qc\]](#).
- [171] T. Damour, N. Deruelle, and R. Ruffini, On Quantum Resonances in Stationary Geometries, *Lett. Nuovo Cim.* **15**, 257 (1976).
- [172] T. J. M. Zouros and D. M. Eardley, INSTABILITIES OF MASSIVE SCALAR PERTURBATIONS OF A ROTATING BLACK HOLE, *Annals Phys.* **118**, 139 (1979).
- [173] S. L. Detweiler, KLEIN-GORDON EQUATION AND ROTATING BLACK HOLES, *Phys. Rev. D* **22**, 2323 (1980).

- [174] R. A. Konoplya and A. Zhidenko, Stability and quasinormal modes of the massive scalar field around Kerr black holes, *Phys. Rev. D* **73**, 124040 (2006), [arXiv:gr-qc/0605013](#).
- [175] R. A. Konoplya and A. Zhidenko, Massive charged scalar field in the Kerr-Newman background I: quasinormal modes, late-time tails and stability, *Phys. Rev. D* **88**, 024054 (2013), [arXiv:1307.1812 \[gr-qc\]](#).
- [176] E. W. Leaver, An Analytic representation of the quasi normal modes of Kerr black holes, *Proc. Roy. Soc. Lond. A* **402**, 285 (1985).
- [177] M. J. Strafuss and G. Khanna, Massive scalar field instability in Kerr spacetime, *Phys. Rev. D* **71**, 024034 (2005), [arXiv:gr-qc/0412023](#).
- [178] S. R. Dolan, Instability of the massive Klein-Gordon field on the Kerr spacetime, *Phys. Rev. D* **76**, 084001 (2007), [arXiv:0705.2880 \[gr-qc\]](#).
- [179] J. G. Rosa, The Extremal black hole bomb, *JHEP* **06**, 015, [arXiv:0912.1780 \[hep-th\]](#).
- [180] S. Hod and O. Hod, Analytic treatment of the black-hole bomb, *Phys. Rev. D* **81**, 061502 (2010), [arXiv:0910.0734 \[gr-qc\]](#).
- [181] S. R. Dolan, Superradiant instabilities of rotating black holes in the time domain, *Phys. Rev. D* **87**, 124026 (2013), [arXiv:1212.1477 \[gr-qc\]](#).
- [182] H. Furuhashi and Y. Nambu, Instability of massive scalar fields in Kerr-Newman space-time, *Prog. Theor. Phys.* **112**, 983 (2004), [arXiv:gr-qc/0402037](#).
- [183] Y. Huang and D.-J. Liu, Scalar clouds and the superradiant instability regime of Kerr-Newman black hole, *Phys. Rev. D* **94**, 064030 (2016), [arXiv:1606.08913 \[gr-qc\]](#).
- [184] Y. Huang, D.-J. Liu, X.-h. Zhai, and X.-z. Li, Instability for massive scalar fields in Kerr-Newman spacetime, *Phys. Rev. D* **98**, 025021 (2018), [arXiv:1807.06263 \[gr-qc\]](#).
- [185] H. S. Vieira, V. B. Bezerra, and C. R. Muniz, Instability of the charged massive scalar field on the Kerr–Newman black hole spacetime, *Eur. Phys. J. C* **82**, 932 (2022), [arXiv:2107.02562 \[gr-qc\]](#).
- [186] P. H. C. Siqueira and M. Richartz, Quasinormal modes, quasibound states, scalar clouds, and superradiant instabilities of a Kerr-like black hole, *Phys. Rev. D* **106**, 024046 (2022), [arXiv:2205.00556 \[gr-qc\]](#).
- [187] D. Liu, Y. Yang, A. Övgün, Z.-W. Long, and Z. Xu, Gravitational ringing and superradiant instabilities of the Kerr-like black holes in a dark matter halo, *Eur. Phys. J. C* **83**, 565 (2023), [arXiv:2204.11563 \[gr-qc\]](#).
- [188] A. Ghosh, R. Brito, and A. Buonanno, Constraints on quasinormal-mode frequencies with LIGO-Virgo binary–black-hole observations, *Phys. Rev. D* **103**, 124041 (2021), [arXiv:2104.01906 \[gr-qc\]](#).
- [189] A. K. Mishra and S. Chakraborty, Strong cosmic censorship conjecture in higher curvature gravity, *Phys. Rev. D* **101**, 064041 (2020), [arXiv:1911.09855 \[gr-qc\]](#).
- [190] R. A. Konoplya and A. V. Zhidenko, Decay of massive scalar field in a Schwarzschild background, *Phys. Lett. B* **609**, 377 (2005), [arXiv:gr-qc/0411059](#).
- [191] E. Franzin, S. Liberati, and M. Oi, Superradiance in Kerr-like black holes, *Phys. Rev. D* **103**, 104034 (2021), [arXiv:2102.03152 \[gr-qc\]](#).
- [192] S. Hod, Kerr-Newman black holes with stationary charged scalar clouds, *Phys. Rev. D* **90**, 024051 (2014), [arXiv:1406.1179 \[gr-qc\]](#).
- [193] H.-P. Nollert, Quasinormal modes of Schwarzschild black holes: The determination of quasinormal frequencies with very large imaginary parts, *Phys. Rev. D* **47**, 5253 (1993).
- [194] J. L. Jaramillo, R. Panosso Macedo, and L. Al Sheikh, Pseudospectrum and Black Hole Quasinormal Mode Instability, *Phys. Rev. X* **11**, 031003 (2021), [arXiv:2004.06434 \[gr-qc\]](#).
- [195] A. Ohashi and M.-a. Sakagami, Massive quasi-normal mode, *Class. Quant. Grav.* **21**, 3973 (2004), [arXiv:gr-qc/0407009](#).
- [196] R. A. Konoplya, Massive vector field perturbations in the Schwarzschild background: Stability and unusual quasinormal spectrum, *Phys. Rev. D* **73**, 024009 (2006), [arXiv:gr-qc/0509026](#).
- [197] A. Zhidenko, Massive scalar field quasi-normal modes of higher dimensional black holes, *Phys. Rev. D* **74**, 064017 (2006), [arXiv:gr-qc/0607133](#).
- [198] K. D. Kokkotas, R. A. Konoplya, and A. Zhidenko, Bifurcation of the quasinormal spectrum and Zero Damped Modes for rotating dilatonic black holes, *Phys. Rev. D* **92**, 064022 (2015), [arXiv:1507.05649 \[gr-qc\]](#).
- [199] S. Hod, Quasi-Bound States of Massive Scalar Fields in the Kerr Black-Hole Spacetime: Beyond the Hydrogenic Approximation, *Phys. Lett. B* **749**, 167 (2015), [arXiv:1510.05649 \[gr-qc\]](#).
- [200] S. Hod, Slowly decaying resonances of charged massive scalar fields in the Reissner-Nordström black-hole spacetime, *Phys. Lett. B* **761**, 53 (2016), [arXiv:1609.01297 \[gr-qc\]](#).
- [201] R. A. Konoplya and A. Zhidenko, Quasinormal modes of massive fermions in Kerr spacetime: Long-lived modes and the fine structure, *Phys. Rev. D* **97**, 084034 (2018), [arXiv:1712.06667 \[gr-qc\]](#).
- [202] R. A. Konoplya, A. F. Zinhailo, and Z. Stuchlík, Quasinormal modes, scattering, and Hawking radiation in the vicinity of an Einstein-dilaton-Gauss-Bonnet black hole, *Phys. Rev. D* **99**, 124042 (2019), [arXiv:1903.03483 \[gr-qc\]](#).
- [203] M. S. Churilova, R. A. Konoplya, and A. Zhidenko, Arbitrarily long-lived quasinormal modes in a worm-hole background, *Phys. Lett. B* **802**, 135207 (2020), [arXiv:1911.05246 \[gr-qc\]](#).
- [204] J. Percival and S. R. Dolan, Quasinormal modes of massive vector fields on the Kerr spacetime, *Phys. Rev. D* **102**, 104055 (2020), [arXiv:2008.10621 \[gr-qc\]](#).
- [205] W. Xiong, P. Liu, C.-Y. Zhang, and C. Niu, Quasinormal modes of the Einstein-Maxwell-aether black hole, *Phys. Rev. D* **106**, 064057 (2022), [arXiv:2112.12523 \[gr-qc\]](#).
- [206] H. Yang, F. Zhang, A. Zimmerman, D. A. Nichols, E. Berti, and Y. Chen, Branching of quasinormal modes for nearly extremal Kerr black holes, *Phys. Rev. D* **87**, 041502 (2013), [arXiv:1212.3271 \[gr-qc\]](#).
- [207] H. Yang, A. Zimmerman, A. Zenginoğlu, F. Zhang, E. Berti, and Y. Chen, Quasinormal modes of nearly extremal Kerr spacetimes: spectrum bifurcation and power-law ringdown, *Phys. Rev. D* **88**, 044047 (2013), [arXiv:1307.8086 \[gr-qc\]](#).
- [208] M. Richartz, Quasinormal modes of extremal black holes, *Phys. Rev. D* **93**, 064062 (2016), [arXiv:1509.04260 \[gr-qc\]](#).

- [209] O. J. C. Dias, M. Godazgar, J. E. Santos, G. Carullo, W. Del Pozzo, and D. Laghi, Eigenvalue repulsions in the quasinormal spectra of the Kerr-Newman black hole, *Phys. Rev. D* **105**, 084044 (2022), [arXiv:2109.13949 \[gr-qc\]](#).
- [210] O. J. C. Dias, M. Godazgar, and J. E. Santos, Eigenvalue repulsions and quasinormal mode spectra of Kerr-Newman: an extended study, *JHEP* **07**, 076, [arXiv:2205.13072 \[gr-qc\]](#).
- [211] S. Sarkar, M. Rahman, and S. Chakraborty, Perturbing the perturbed: Stability of quasinormal modes in presence of a positive cosmological constant, *Phys. Rev. D* **108**, 104002 (2023), [arXiv:2304.06829 \[gr-qc\]](#).
- [212] J. C. S. Neves and C. Molina, Rotating black holes in a Randall-Sundrum brane with a cosmological constant, *Phys. Rev. D* **86**, 124047 (2012), [arXiv:1211.2848 \[gr-qc\]](#).
- [213] D. Baumann, G. Bertone, J. Stout, and G. M. Tomaselli, Sharp Signals of Boson Clouds in Black Hole Binary Inspirals, *Phys. Rev. Lett.* **128**, 221102 (2022), [arXiv:2206.01212 \[gr-qc\]](#).
- [214] G. M. Tomaselli, T. F. M. Spieksma, and G. Bertone, Dynamical friction in gravitational atoms, *JCAP* **07**, 070, [arXiv:2305.15460 \[gr-qc\]](#).
- [215] T. Takahashi, H. Omiya, and T. Tanaka, Axion cloud evaporation during inspiral of black hole binaries: The effects of backreaction and radiation, *PTEP* **2022**, 043E01 (2022), [arXiv:2112.05774 \[gr-qc\]](#).
- [216] T. Takahashi, H. Omiya, and T. Tanaka, Evolution of binary systems accompanying axion clouds in extreme mass ratio inspirals, *Phys. Rev. D* **107**, 103020 (2023), [arXiv:2301.13213 \[gr-qc\]](#).
- [217] J. Zhang and H. Yang, Gravitational floating orbits around hairy black holes, *Phys. Rev. D* **99**, 064018 (2019), [arXiv:1808.02905 \[gr-qc\]](#).
- [218] J. Zhang and H. Yang, Dynamic Signatures of Black Hole Binaries with Superradiant Clouds, *Phys. Rev. D* **101**, 043020 (2020), [arXiv:1907.13582 \[gr-qc\]](#).
- [219] X. Tong, Y. Wang, and H.-Y. Zhu, Termination of superradiance from a binary companion, *Phys. Rev. D* **106**, 043002 (2022), [arXiv:2205.10527 \[gr-qc\]](#).
- [220] K. Fan, X. Tong, Y. Wang, and H.-Y. Zhu, Superradiance Termination: The Cloud Strikes Back, (2023), [arXiv:2311.17013 \[gr-qc\]](#).
- [221] R. Cayuso, O. J. C. Dias, F. Gray, D. Kubizňák, A. Margalit, J. E. Santos, R. Gomes Souza, and L. Thiele, Massive vector fields in Kerr-Newman and Kerr-Sen black hole spacetimes, *JHEP* **04**, 159, [arXiv:1912.08224 \[hep-th\]](#).